DESIGN OF A PHOTOVOLTAIC POWER CONVERTER FOR DRIVING AND CONTROLLING AC MOTORS

HAMED ATYIA SOODI

OCTOBER 2014

DESIGN OF A PHOTOVOLTAIC POWER CONVERTER FOR DRIVING AND CONTROLLING AC MOTORS

A THESIS SUBMITTED TO
THE GRADUATE SCHOOL OF NATURAL AND APPLIED SCIENCES OF
ÇANKAYA UNIVERSITY

BY
HAMED ATYIA SOODI

IN PARTIAL FULFILMENT OF THE REQUIREMENTS FOR THE DEGREE OF
MASTER OF SCIENCE
IN
THE DEPARTMENT OF
ELECTRONIC AND COMMUNICATION ENGINEERING

OCTOBER 2014

Title of the Thesis: **Design of a Photovoltaic Power Converter For Driving and Controlling AC Motors**

Submitted by **Hamed Atyia SOODI**

Approval of the Graduate School of Natural and Applied Sciences, Çankaya University.

Prof. Dr. Taner ALTUNOK
Director

I certify that this thesis satisfies all the requirement as a thesis for the degree of Master of Science.

Prof. Dr. Celal Zaim ÇİL
Head of Department

This is to certify that we have read this thesis and that in our opinion it is fully adequate, in scope and quality, as a thesis for the degree of Master of Science.

Assoc. Prof. Dr. Klaus Werner SCHMIDT
Supervisor

Examination Date: 20.10.2014

Examining Committee Members

Assoc. Prof. Dr. Ulaş BELDEK	(Çankaya Univ.)	
Assoc. Prof. Dr. Klaus Werner SCHMIDT	(Çankaya Univ.)	
Dr. Bora KARTAL	(ODTÜ)	

STATEMENT OF NON-PLAGIARISM PAGE

I hereby declare that all information in this document has been obtained and presented in accordance with academic rules and ethical conduct. I also declare that, as required by these rules and conduct, I have fully cited and referenced all material and results that are not original to this work.

Name, Last Name : **Hamed Atyia SOODI**

Signature :

Date : 20.10.2014

ABSTRACT

DESIGN OF A PHOTOVOLTAIC POWER CONVERTER FOR DRIVING AND CONTROLLING AC MOTORS

SOODI, Hamed Atyia

M.Sc., Department of Electronic and Communication Engineering

Supervisor: Assoc. Prof. Dr. Klaus Werner SCHMIDT

October 2014, 50 pages

The availability of renewable energy sources is of increasing importance on the market. In order to use renewable energy efficiently, suitable power processing equipment is needed to support different applications such as energy storage, feeding energy to the grid or driving AC motors. The subject of this thesis is the power processing for the speed control of AC motors, whereby photovoltaic (PV) modules are considered as the renewable energy source. In the classical design, this task is performed in two stages. First, the low DC voltage provided by the PV module is boosted to a higher voltage level that is suitable for driving the AC motor using a DC-DC converter. Second, the resulting DC link voltage is converted to a 3-phase AC voltage that is used for driving the AC motor by the help of a voltage source inverter (VSI). The frequency of this AC can be changed in order to change the motor speed. In contrast, this thesis proposes to employ a Z-source inverter (ZSI) as an AC motor drive. The ZSI combines the DC voltage boost and the AC voltage generation in a single stage by using a special capacitor/inductor network. The thesis first provides the model of the ZSI and discusses the working principle of voltage boost. Then, the generation of a variable frequency AC voltage based on the space-vector the pulse width modulation is elaborated. Together, a complete design of a VSI for driving AC motors is obtained. The suitability of the design is evaluated by a

simulation study in Matlab/Simulink. It shows that the designed VSI can be optimized for AC motors with different characteristics. In addition, it is verified that the same VSI can be used for different AC motors by simply adjusting the voltage boost, that is, without changing any hardware components.

Keywords: Power Electronics, Inverter, AC Motor, Z-Source, Space-Vector Modulation, Simulation.

ÖZ

AC MOTORLARIN SÜRÜLMESİ VE KONTROL EDİLMESİ İÇİN BİR FOTOVOLTAİK GÜÇ ÇEVİRİCİ TASARIMI

SOODI, Hamed Atyia

Yüksek Lisans, Elektronik ve Haberleşme Mühendisliği Anabilim Dalı

Tez Yöneticisi: Doç Dr. Klaus Werner SCHMIDT

Ekim 2014, 50 sayfa

Yenilenebilir enerji kaynaklarının mevcudiyeti piyasada artarak önem arzetmeye devam etmektedir. Yenilenebilir enerjinin verimli bir şekilde kullanılabilmesi için, enerji depolanması, şebekeye enerjinin beslenmesi ve AC motorların sürülmesi gibi farklı uygulamaların desteklendiği uygun güç işleme ekipmanları gerekmektedir. Bu tezin konusu fotovoltaik modüllerin yenilebilir enerji kaynağı olarak kullanıldığı durumda elde edilen gücün AC motorların hız kontrolü amacıyla işlenmesidir.

Kasikik bir tasarımda bu görev iki aşamada gerçekleştirilir. İlk önce, fotovoltailk modülden elde edilen DC voltajı, AC motoru sürmeye uygun daha yüksek bir DC voltaj seviyesine DC-DC çevirici kullanılarak yükseltilir. Daha sonra, elde edilen yükseltilmiş DC voltaj seviyesi 3 faz AC voltaja çevrilir ve bu 3 faz AC voltaj voltaj-kaynak çevirici devresi kullanılarak AC motor sürülür. AC motoron hızını elde edilen AC voltajın frekansını ayarlayarak değiştirilebilir.

Klasik tasarımın aksine bu tezde AC motoroun sürülmesi için Z-kaynak çevirici devresine başvurulması önerilmiştir. Z-kaynak devresi özel bir kondansatör - inductor devresi kullanarak DC voltaj yükseltilmesini ve AC voltaj üretimini (dönüşümünün) tek bir aşamada birleştirir**.** Bu tez ilk once Z-kaynak devresinin modelini sağlamakta ve bu devrenin çalışma prensibin anlatmaktadır. Daha sonra,

uzay-vektör darbe genişliği kiplenimi tabanlı değişken frekanslı AC voltajının üretilmesi ayrıntılı biçimde ele alınmıştır. Bu aşamalar birleştirilerek AC motorları sürmek amacıyla tam bir voltaj-kaynak çevirici devre tasarımı elde edilmiştir.

Tasarımın uygunluğu MATLAB/Simulink'te gerçekleştirilen benzetim uygulamalarıyla gerçekleştirilmiştir. Bu benzetimlerde farklı karakteristiklere sahip AC motorlarında tasarlanan voltaj-kaynak çevirici devrelerinin optimize edilebileceği (eniyilenebileceği) görülmüştür. Buna ek olarak, aynı voltaj-kaynak çevirici devresinin donanım birimlerini değiştirmeden sadece basitçe voltaj yükseltme kısmını ayarlayarak farklı AC motorlarına kullanılabileceği doğrulanmıştır.

Anahtar Kelimeler: Serpiştirilmiş Kodlanmış Sistemler, Uzay Zaman Kodlama, Birleşik Yapılar, İşbirlikli Sistemler, Yinelemeli Çözüm.

ACKNOWLEDGEMENTS

I would like to express my sincere gratitude to my thesis advisor Assoc. Prof. Dr. Klaus Werner SCHMIDT, who has encouraged and guided me throughout this thesis patiently.

I also would like to express my deepest gratitude to my ill mother for her support and encouragement and her prayers that make me successful and hopeful in the life. To my father whose support makes my way of success .To my dearest and lovely sister and brother.

I also would like to express my sincere gratitude to my dear wife, for her continuous support and being with me in both my good and hard times.

I also would like to express my gratitude to the Iraqi ministry of electrical as well as to Dibis electrical power station for their cooperation.

Finally, I thank Çankaya University precisely Mechatronics Engineering Department, as well as Electronic and Communication Engineering Department, for their support.

TABLE OF CONTENTS

Page

CHAPTERS

LIST OF FIGURES

FIGURES **Page**

FIGURES **Page**

LIST OF TABLES

LIST OF ABBREVIATIONS

ZSI	Z-Source Inverter
ZSC	Z-Source Converter
VSI	Voltage Source Inverter
PV	Photo Voltaic
CSI	Current Source Inverter
PWM	Pulse Width Modulation
SVM	Space Vector Modulation
SVPWM	Space Vector Pulse Width Modulation
SPWM	Sinusoidal Pulse Width Modulation
MSVPWM	Modify Space Vector Pulse Width Modulation
ASD	Adjustable Speed Driver

CHAPTER 1

INTRODUCTION

AC motors are frequently used in industry because of their robustness, reliability, low prices and high efficiency (up to 80%) [1, 2, 3]. The characteristics of different AC motors differ in the maximum speed and torque values that can be achieved. In principle, AC motors are operated by applying a 3-phase AC power supply, whereby the input voltage amplitude depends on the respective AC motor characteristics. Varying the frequency of the input voltage supply allows changing the motor speed. The 3-phase AC voltage is usually provided by a power processing equipment denoted as AC drive that converts a certain form of input power to the required 3-phase AC voltage.

In the recent years, the usage of renewable energy becomes increasingly important. In this thesis, the usage of photovoltaic (PV) modules as input power source for AC-drives is considered. The classical schematic of such AC motor control system is shown in Fig. 1. Since the PV module usually provides a low voltage, a DC-DC converter is used to boost the voltage to a higher value of the DC-link voltage that is suitable for the AC motor. Then, an inverter converts the DC-link voltage to a 3-phase AC voltage that can be connected to the AC motor. A disadvantage of this design is the additional DC-DC converter stage that is needed to boost the DC voltage of the PV panel. In addition, the voltage is boosted to a fixed value such that such inverter system can only be used for

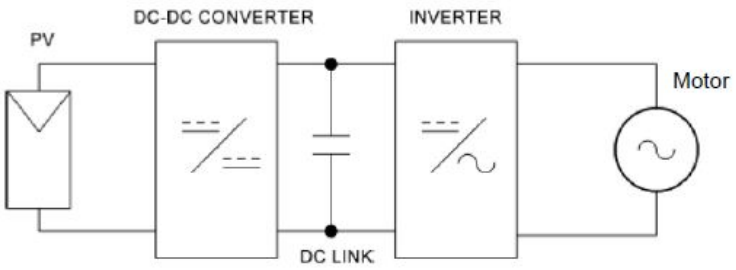

Figure 1: AC motor system with PV panel, DC-DC converter and inverter

AC motors with a certain input voltage amplitude.

The main subject of this thesis is the realization of the AC-drive by a particular Z-source network [4, 5]. The resulting Z-source inverter (ZSI) is shown in Fig. 2. It comprises

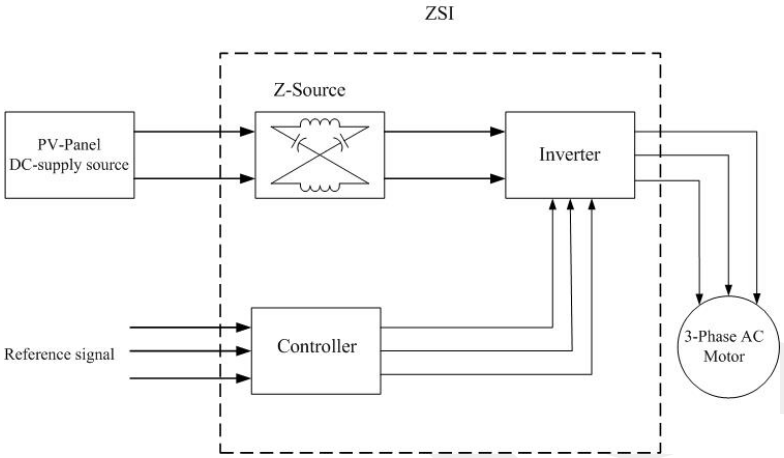

Figure 2: AC motor drive using ZSI and PV module.

two inductors and capacitors connected in an X-shape that are connected to a 3-phase inverter bridge. The main advantage of the ZSI is that it combines the DC-DC voltage boost and the AC voltage generation in a single stage [6]. In addition, the amount of voltage boost can be adjusted in software without needing any hardware modifications. Hence, the same ZSI design can be used for different AC motors with different voltage requirements. Finally, the ZSI can be applied to areas where the DC input voltage is unreliable or shows large variations such as in photovoltaic systems and full cell applications. We note that, although the Z-source is used for driving an AC motor in this thesis, it can as well be used for other applications such as feeding power to the power grid.

Using this basic structure of the ZSI, the main contributions of this thesis are as follows:

- Determination of the model equations of the Z-source inverter for AC motors based on the existing literature [7],
- Derivation of the design equations needed for voltage boost;
- Realization of space-vector pulse-width modulation (SVPWM) in order to generate appropriate AC voltages [8],
- Implementation of the ZSI in Simulink and evaluation of the boost capabilities
- Usage of the designed SVPWM AC motor control,

- Implementation of the AC motor control with ZSI in Simulink,
- The main novelty is a comparative study of different ZSI designs for AC motors with different characteristics. It is shown that the same ZSI design can be used for different AC motors due to the voltage boost capabilities. It is further shown that the Z-source can compensate variations in the input DC voltage level.

The organization of the thesis is as follows. Chapter 2 gives background information about PV modules, inverters, space vector modulation and AC motors. The design of inverters that use the Z-source network is discussed in Chapter 3. In particular, model equations and design guidelines are given. Chapter 4 provides our results on the usage of the ZSI for AC motor control including an extensive simulation study. Conclusions and ideas for future work are given in Chapter 5.

CHAPTER 2

BACKGROUND

2.1 PV Module

Photovoltaic modules are used to convert solar energy from the sun to electrical energy. Solar cell power generation is a clean energy that relies on the sun as a widely distributed source of renewable energy. A photovoltaic panel usually consists of many photovoltaic cells connected in series (cell string) and protected by a diode as shown in Fig. 3. A photovoltaic cell is a semiconductor diode (p-n) junction which converts the solar energy to electrical energy. Different materials such as polycrystalline silicon, mono-crystalline silicon, micro-crystalline silicon, copper indium seleucid or cadmium telluride can be used to manufacture solar cells.

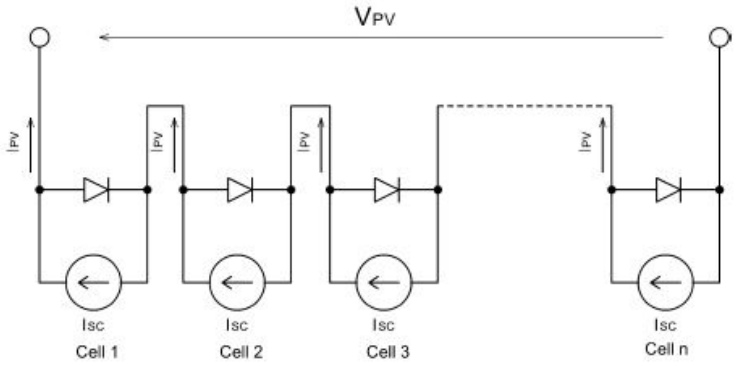

Figure 3: Multiple cell of PV panel series connection

The output voltage and output current of a solar module depend on the solar irradiation, cell temperature and the material of the photovoltaic cell. For example, increase in the cell temperature to a high level reduces the output voltage and the output power. The characteristics of a solar cell are shown in Fig. 4.

Here, the fundamental parameters related to solar cell are the short circuit current I_{sc},

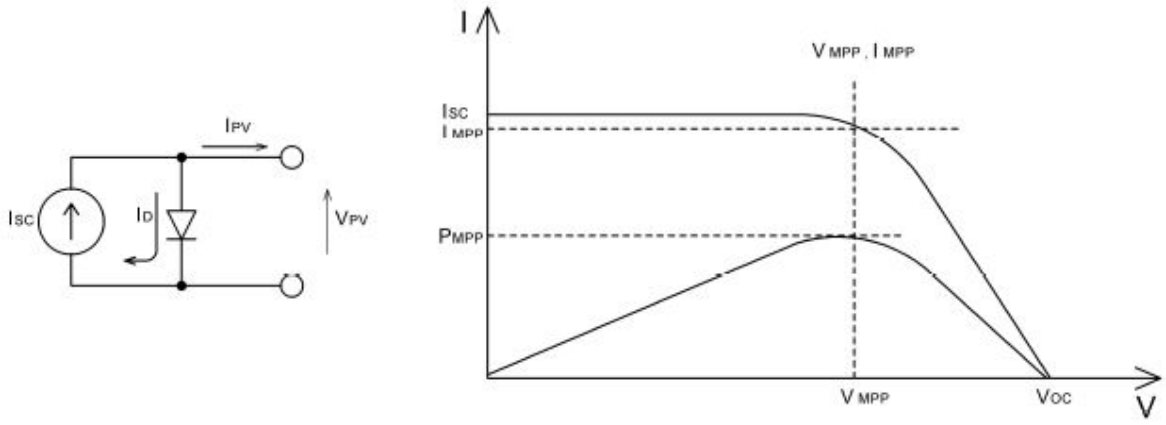

Figure 4: Characteristic of solar cell

the open circuit voltage V_{oc} and the maximum power point MPP. It holds that

$$I_{atv=0} = I_{sc} \tag{2.1}$$

$$Pmax = V_{MPP} \cdot I_{MPP} \tag{2.2}$$

$$P_{max} = V_{oc} \cdot I_{sc} * FF \tag{2.3}$$

where FF is the Fill Factor, also known as curve factor that measures the squareness in the $I-V$ curve. In order to maximize the power obtained from a solar module, it is desired to operate the module in the MPP. [9], [10],[11] give more details and information about photovoltaic characteristics and tracking the MPP.

2.2 The Inverter (DC/AC Converter)

The purpose of a DC/AC converter (inverter) is the conversion of direct current to alternating current. Fig. 5 shows a typical DC/AC converter (inverter) system. There are two types of inverters: single phase inverters and three phase inverters. The input is provided by a DC current or voltage source and the output is desired to be a sinusoidal current or voltage without DC component. The load can be an R-L-C circuit, an AC current or AC voltage sink.

The basic structure of a single phase inverter is shown in Fig. 6 (a). The single phase DC/AC conversion is achieved by opening and closing the diagonal switch pairs S2-S3 or S1-S4 alternately. The resulting output voltage waveform is shown in Fig. 6 (b). The input voltage and its negative counterpart are visible at the output depending on the

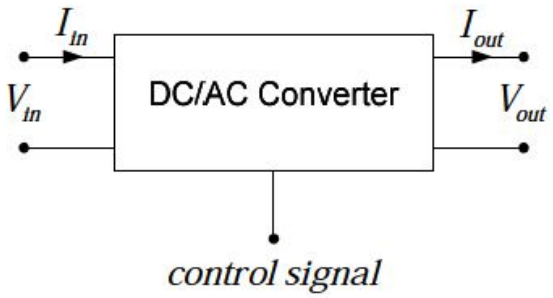

Figure 5: Inverter block diagram

switch states.

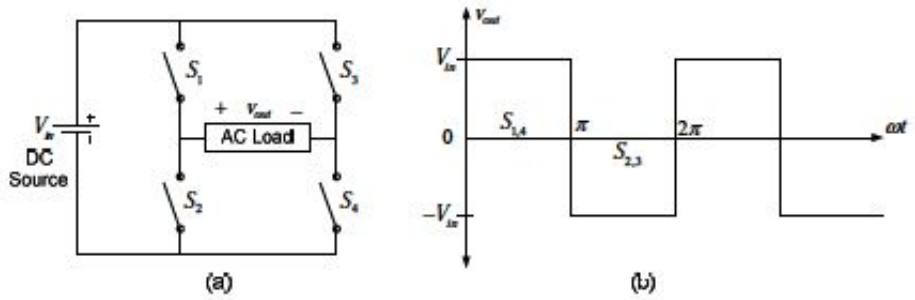

Figure 6: (a) Single phase inverter; (b) Output AC voltage

The zero state is one of the common ways of varying the AC voltage parameters. The zero state is obtained by closing all the upper switches (S1-S3) or the lower switches (S2-S4). Fig. 7 (a) shows the output voltage of the single phase inverter by using the zero state of varying the AC voltage parameters.

The Pulse Width Modulation (PWM) technique is also very commonly used in inverter for changing the parameters of the AC voltage. In this technique, using high frequency switching, it is possible to remove undesirable low frequency harmonics and to filter the high frequency switching harmonics. The AC output voltage wave of the single phase inverter by using PWM technique is shown in Fig. 7 (b).

Most of the applications in industry such as AC motor controls need a three phase AC source with variable frequency. A three phase inverter can be obtained by replacing the single phase bridge with a three phase bridge as is shown in Fig. 8 (a). Fig. 8 part (b) shows the phase to phase output voltage of such three phase inverter when the lower and upper leg switches are opened and closed accordingly.

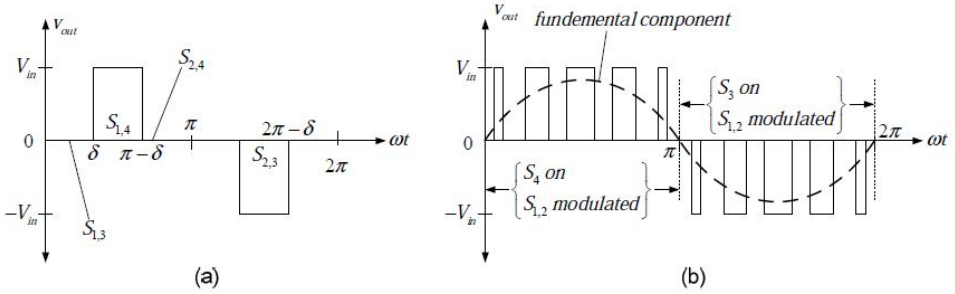

Figure 7: (a)Output voltage with zero state;(b)Output voltage with PWM

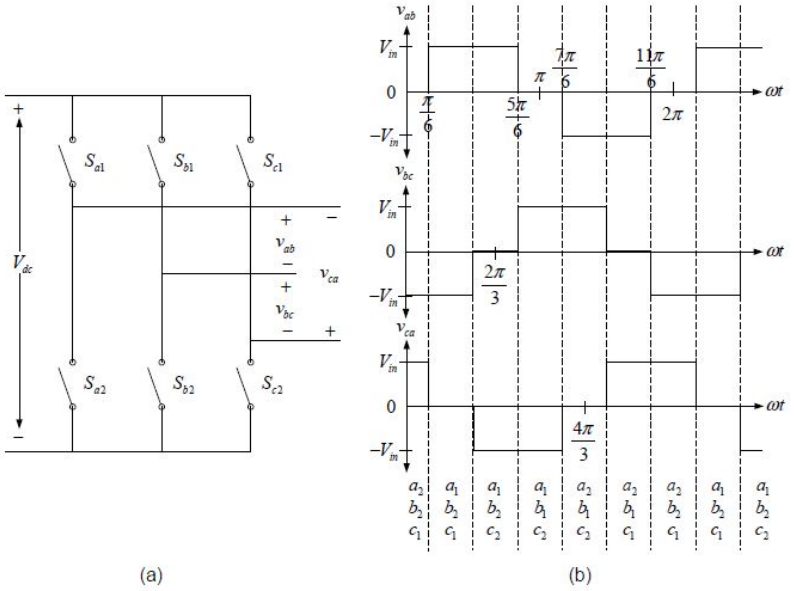

Figure 8: (a)Three phase inverter; (b) Output voltage and switch positions

There are two basic types of DC/AC converters denoted as current source inverter (CSI) and voltage source inverter (VSI) as shown in Fig. 9. The VSI is fed by a DC voltage source and supported by a large capacitor. The DC voltage source can be a solar module, fuel cell, battery or AC/DC converter. The bridge cascaded to the source consists of switches with anti-parallel diode which enables bidirectional current flow and unidirectional voltage. Similarly, for the CSI, the large inductor is placed in series with the DC voltage source and the switches is series with diodes provide unidirectional current and bidirectional voltage,[12],[13] give as more dateless about DC to AC converter.

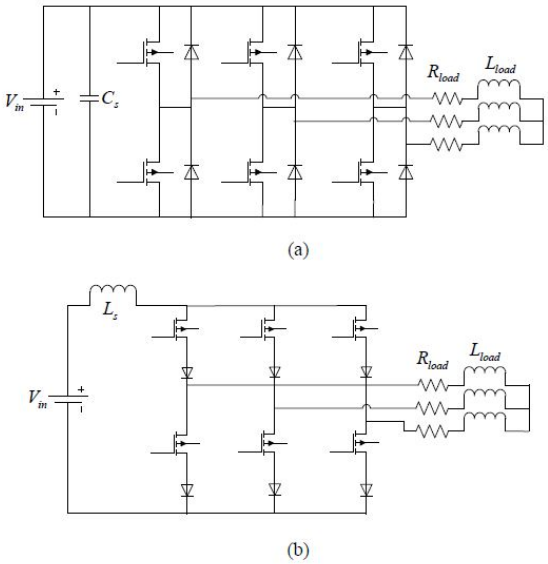

Figure 9: Three phase inverters: (a) VSI (b) CSI

VSIs are for example used in power supply (UPS), adjustable speed drives (ASD) for AC motor and electronic frequency changer. Both VSI and CSI have some of the following conceptual theoretical limitations which makes it difficult to use them without additional circuitry.

1. For VSI, the AC output voltage is limited below the DC input voltage and cannot boost the DC input voltage without additional circuitry. The CSI is the boost inverter such that the AC output current is greater than the AC input current but it cannot be used as buck converter.

2. For VSI, the upper and lower switch for each leg cannot be on at the same time in order to avoid short circuit. For the CSI, the upper switch and one switch from any leg have to be on to satisfy the continuous input current.

3. The VSI needs switches with anti-parallel diodes. On the other hand, the CSI

needs switches with diodes in series which cause a higher cost of CSI.

2.3 Space Vector Modulation

Space Vector Modulation (SVM) today becomes a well-established method for switching power converter systems. Initially, SVM was used for the three phase voltage source inverter and was afterward also applied to three phase as AC/DC or DC/AC current source converters.

The operation principle of SVM is based on the characteristics of any three phase waveform. Consider V_a, V_b and V_c as three phase voltage components that are displaced by a phase difference of 120 degrees:

$$V_a = V_m sinwt \tag{2.4}$$

$$V_b = V_m sin(wt - 120) \tag{2.5}$$

$$V_c = V_m sin(wt - 240) \tag{2.6}$$

These three vectors can be represented uniquely by a rotating vector which is know as space vector

$$V_s = V_a + V_b \cdot e^{j2pi/3} + V_c \cdot e^{-j2\pi/3} \tag{2.7}$$

$$V_s = 3/2 \cdot V_m[sinwt - jcoswt] \tag{2.8}$$

This vector has a magnitude of $3/2V_m$ and rotates in space at a frequency of w rad/sec as shown in Fig. 10.

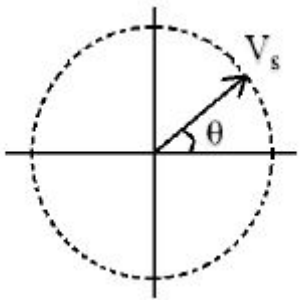

Figure 10: Rotation of the space vector

Given a three-phase system, a vectorial representation is achieved by the dq transformation

$$\begin{bmatrix} V_d \\ V_q \end{bmatrix} = 2/3V_{dc} \cdot \begin{bmatrix} 1 & -1/2 & -1/2 \\ 0 & \sqrt{3}/2 & -\sqrt{3}/2 \end{bmatrix} \begin{bmatrix} V_a \\ V_b \\ V_c \end{bmatrix} \tag{2.9}$$

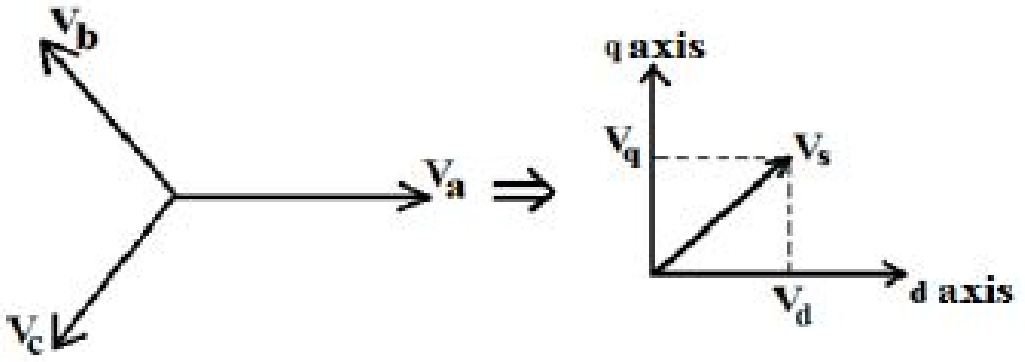

Figure 11: Transformation of the abc axis to the dq axis

The advantage of this mathematical representation is:

- Analysis of three phase system in total instead of looking at each phase separately,
- Possibility to use the properties of the vectorial rotation. Using rotation with *wt* leads to an analysis in DC components.

This vectorial representation is the fundamental of the control algorithm for:

- electrical drives, synchronous machine drives and induction machines,
- AC/DC or DC/AC converters,
- Active filtering systems depended on the instantaneous power components ($p-q$ theory).

2.3.1 The principle of space vector PWM (SVPWM)

The control of the electric power is performed by using power converters. Energy is transferred from the source in a mode of switching operation that ensures high conversion efficiency. The algorithms that generates the switching function are called Pulse-Width Modulation (PWM) techniques. The purpose of SVPWM is to generate a voltage near to the reference circle using the switching modes of the inverter.

The Pulse Width Modulation controls the average output voltage over a small enough time period called switching period through the production of the variable duty cycle pulse. The switching period signal is small compared with the periodic desired output signal, so that the output voltage can be considered equal to the desired signal.

The popular PWM techniques are the sinusoidal pulse width modulation and space vector pulse width modulation [14],[15]. Fig. 12 displays the concept of sinusoidal pulse width modulation. The triangular wave with the high frequency is called the carrier wave, the sinusoidal signal represents the desired output signal (reference signal). The comparator compares the carrier signal and reference signal and produces the output signal which turns on and turn off the lower power transistor switch.

The ratio of $m_{triangular} = magnitude_{reference}/magnitude_{carrier}$ is called the modulation index. The maximum output voltage that can be obtained by using the sinusoidal pulse width modulation is $1/2 \cdot V_{dc}$ with modulation index not exceeding unity.

The space vector modulation (SVM) has become the most important pulse width modulation technique for three phase voltage inverters and is also a standard for the switching power converters. In (SVM) the rotating reference signal in each switching cycle operates by switching between two nearest non-zero states (active vector) and the zero state (null vector) so as to maintain the effective switch frequency of the power transistor switching at minimum.

Fig. 13 shows the typical diagram of a three phase inverter. There are six switches (S1 to S6) that can shape the output voltage. They are controlled by switching variables (a,a',b,b',c,c') . When the upper power transistor is switched on by given a,b,or c equal to 1,the corresponding lower power transistor is switched off by given a', b' or c' equal to 0.

For this model we have 8 possible switch states, six of this state are active state because a voltage is applied to the motor – (1,0,0),(0,0,1),(1,1,0),(0,1,1),(0.1.0),(1,0,1),

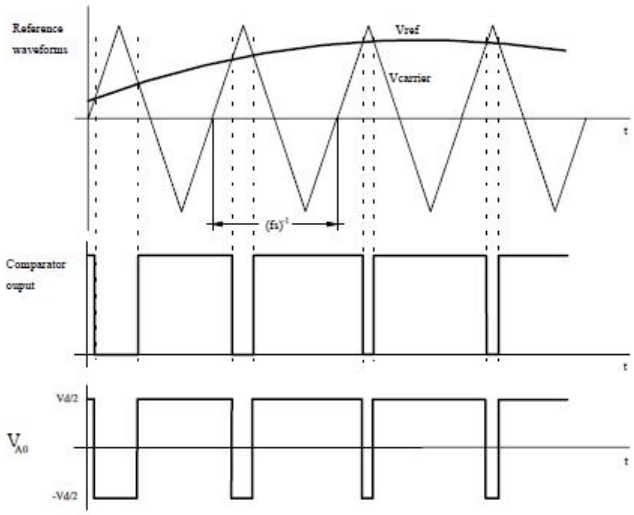

Figure 12: Sinusoidal pulse width modulation

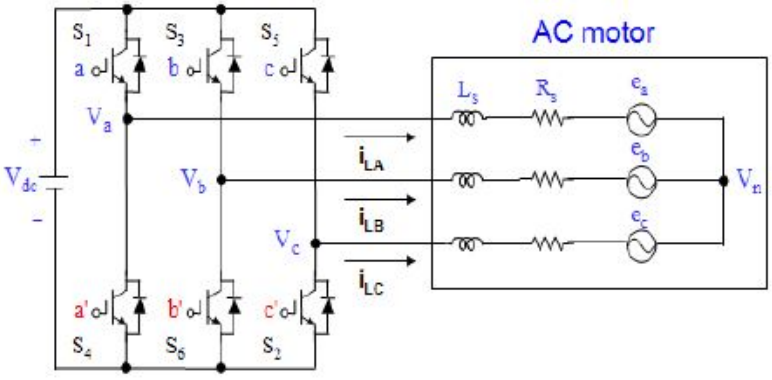

Figure 13: Three phase voltage PWM inverter with AC motor

and there are two zero states when the voltage applied to motor is zero.

The main steps for the space vector PWM is realized depended on the following steps

1. Determine V_d, V_q and the angle for each switching state.
2. Determine the switching time duration at all six sectors.
3. Determine the switching time at each power transistor switching (S1 to S6).

(A) For Step1

The relationship between the power transistor switching state and the phase voltage vector is given in

$$\begin{bmatrix} V_{an} \\ V_{bn} \\ V_{cn} \end{bmatrix} = 1/3 \cdot V_{dc} \begin{bmatrix} 2 & -1 & -1 \\ -1 & 2 & -1 \\ -1 & -1 & 2 \end{bmatrix} \begin{bmatrix} a \\ b \\ c \end{bmatrix} \tag{2.10}$$

$$\begin{bmatrix} V_d \\ V_q \end{bmatrix} = V_{dc} \cdot \begin{bmatrix} \sqrt{6}/3 & -1/\sqrt{6} & -1/\sqrt{6} \\ 0 & 1/\sqrt{2} & -1/\sqrt{2} \end{bmatrix} \begin{bmatrix} a \\ b \\ c \end{bmatrix} \tag{2.11}$$

$$V_{ref} = \sqrt{V_d^2 + V_q^2} \tag{2.12}$$

$$\alpha = \tan^{-1}(V_q/V_d) \tag{2.13}$$

We next derive the magnitude with angle of the possible switching states.

- For(0,0,0):$V_0 = V_s = 0\angle 0$
- For(1,0,0):$V_1 = V_s = V_{dc}\angle 0$
- For(1,1,0):$V_2 = V_s = V_{dc}\angle 60$
- For(0,1,0):$V_3 = V_s = V_{dc}\angle 120$
- For(0,1,1):$V_4 = V_s = V_{dc}\angle 180$
- For(0,0,1):$V_5 = V_s = V_{dc}\angle 240$
- For(1,0,1):$V_6 = V_s = V_{dc}\angle 300$
- For(1,1,1):$V_7 = V_s = 0\angle 0$

As shown in the above equation there are six active vectors (V1 to V6) and two zero vectors (V0 and V7). Table 1 summarizes the switching vectors along with the corresponding line to line voltage and line to neutral voltage applied to the motor.

Table 1: Switching States and Output Voltage of Three-Phase VSI

Voltage Vectors	Switching Vectors			Line To Natural Voltages			Line To Line Voltages		
	a	b	c	V_a	V_b	V_c	V_{ab}	V_{ba}	V_{ca}
V0	0	0	0	0	0	0	0	0	0
V1	1	0	0	2/3	-1/3	-1/3	1	0	-1
V2	1	1	0	1/3	1/3	-2/3	0	1	-1
V3	0	1	0	-1/3	2/3	-1/3	-1	1	0
V4	0	1	1	-2/3	1/3	1/3	-1	0	1
V5	0	0	1	-1/3	-1/3	2/3	0	-1	1
V6	1	0	1	1/3	-2/3	1/3	1	-1	0
V7	1	1	1	0	0	0	0	0	0

Note that each of the respective voltages should be multiplied by V_{dc} while plotting the 8 voltage vectors V_0 to V_7 in the complex plane. This is shown in Fig. 14. The angle between any two non- zero vectors for the active state is equal to 60 degrees and the two zero vectors for the zero states is the origin.

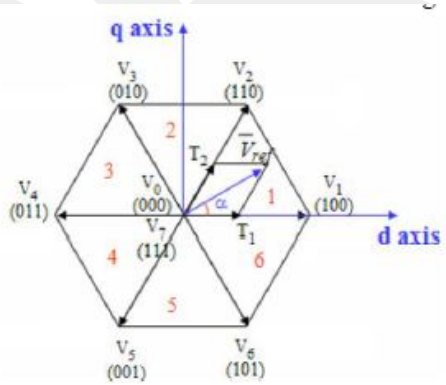

Figure 14: The basic switching vector with sectors

(B) For step two, determine time durations T0,T1,T2

It is considered that the active voltage vectors divide the complex plane in 6 sectors as is shown in Fig. 14.. By using the space vector PWM technique, the desired space vector in a certain sector is synthesized by averaging over two adjacent active vectors and the null vector.

For sector 1, Fig. 15 shows the calculation of the time duration according to voltage-sec principle.

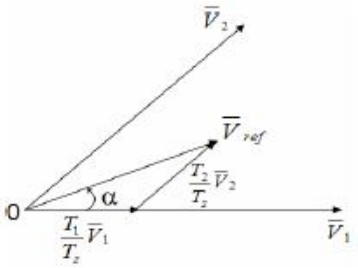

Figure 15: Reference with time duration

$$T1 = T_z \cdot |V_{ref}|/V_{dc} \cdot \sin(\pi/3 - \alpha)/\sin(\pi/3) \tag{2.14}$$

$$T2 = T_z \cdot |V_{ref}|/V_{dc} \cdot \sin(\alpha)/\sin(\pi/3) \tag{2.15}$$

$$T0 = T_z - (T1 + T2) \tag{2.16}$$

$$T_z = T_s/2 \tag{2.17}$$

In these equations, $0 \leq \alpha \leq 60$, T1 represents the time for which $V1$ is applied, T2 represents the time for which $V2$ is applied, T0 represents the time for which null vector ($V0 and V7$) is applied, Ts represents the sampling time.

Similarly, the magnitude and the angle (α) can be calculated for the other sectors.

(C) For step three, determine the switching time for each power switch transistor (S1 to S6).

The space vector pulse modulation has a symmetrical pulse pattern with two non-active states (zero state) that are distributed equally on both ends of the active state as shown in Fig. 16.

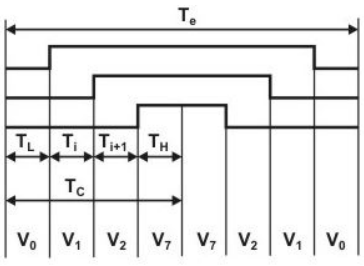

Figure 16: Symmetrical pulse pattern

2.3.2 Advantages of SVPWM compared to SPWM

The advantages of SVPWM compared to SPWM are listed as follows.

- The output voltage which is produced in case of SVPWM is about 15 percent higher than in case of SPWM.
- In SPWM different phase legs may switch at the same time. Only one phase legs switches at a time in case of SVPWM which reduces switching losses compared with SPWM .
- In case of SVPWM is less amount of current and voltage harmonics than in case of SPWM because it has higher modulation index compared to SPWM.

2.4 AC Motor

The AC motors are the important part for any electrical system. They convert the electrical energy to mechanical energy and hence provide an interface facility between the electrical and mechanical system. Any motor generally consists of two parts. The stationary part and rotating part, which have two types of windings: armature windings for the power applied and field windings which produce the magnetic field. The interaction between the magnetic field and the field from armature produces the torque and this torque causes the rotor to rotate.

Today the AC motor use may be divided into two main categories: synchronous and asynchronous (induction) motors. These two types of motor differ according to how the rotor field excitation works. For induction motors, the current is induced into the rotor winding according to rotating stator magnetic field and there is no external applied rotor excitation. For synchronous motors, a DC field excitation is applied to the field winding on the rotor from external source. This difference in field excitation leads to differences in motor characteristics.

2.5 Adjust Speed Drive (ASD)

Adjustable speed drive (ASD) describes equipment which is used to control the speed of motor. Many industrial processes such as a flow, pressure and assembly lines operate

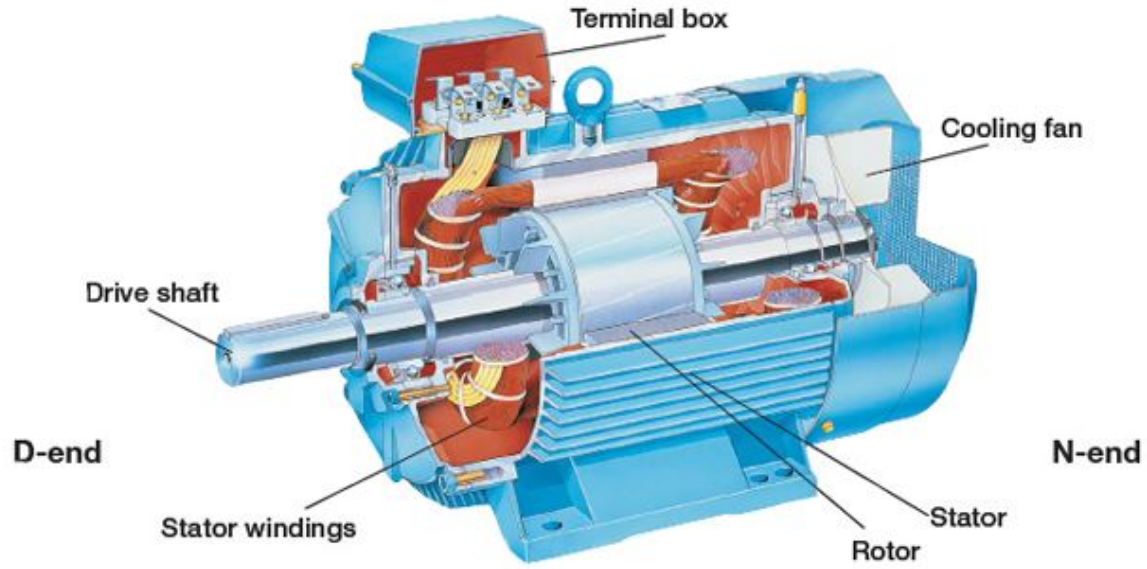

Figure 17: The AC motor

at different speeds which have varying output requirement . Energy conversion and the process control are the primary reasons for using an adjustable speed drive but another important objective can be achievable by using adjustable speed drive such as,'torque control, acceleration control, smoother operation, production rate adjustment,reverse operation ,elimination of mechanical drive components' . There are three types of drives, AC drive, DC drive and Eddy current drive[16],[17].

The AC induction motors are the most widely used in industrial for general purposes because of the following properties : good speed regulation, higher power factor and self starting. The AC motor can operate at fixed speed by determining the number of poles and the frequency for voltage source supply. The synchronous speed is defined by the equation.

$$N_s = 120/p \cdot f \tag{2.18}$$

$$W_s = 4\pi/P \cdot f \tag{2.19}$$

$$N_r = (1-S)N_s \tag{2.20}$$

$$S = N_s - N_r/N_s \tag{2.21}$$

N_s is the synchronous speed in rpm, f is the frequency in Hz, p is the number of poles of the stator of motor, W_s is the synchronous speed in rad/sec, N_r is the rotor speed, S is the slip coefficient

There are many methods for speed control of induction motor, [18].

- Stator voltage control.
- Stator current control.
- stator frequency control.
- Slip power recovery control .
- V/F control(scalar control).

Since the number of poles is fixed in the motor at design, one of the best ways to control the speed of motor is to change the supply frequency f and the torque developed by the motor is directly proportional to the ratio of the voltage V to the frequency for supply source. Keeping the torque constant is achievable by changing the applied voltage and supply frequency and by keeping the ratio of (V/F) to constant value.

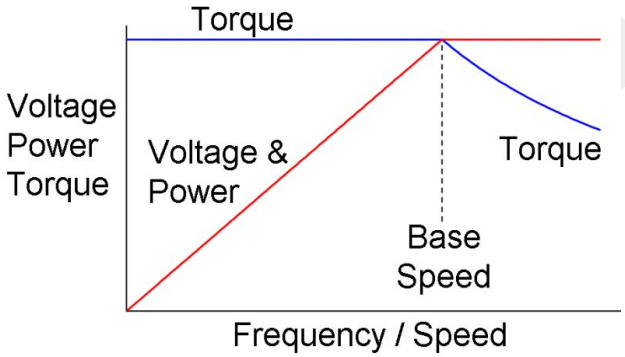

Figure 18: V/F ratio

CHAPTER 3

POWER CONVERTER WITH VOLTAGE BOOST

3.1 Introduction

High performance current source and voltage source inverters (CSI and VSI) are the most important equipment in components for various DC/AC applications such as hybrid electric vehicles, servo motor drives, power supplies and distributed power system. However with ever increase energy requirement, the traditional voltage source inverter (VSI) and current source inverter (CSI) show serious limitations according to their narrow obtainable output voltage range [19]. The z-source inverter (ZSI) is one of the new promising topology conversion sources [20]. The most common application of Z-source inverter (ZSI) is the DC/AC conversion (inverter) but can also be applied to AC/AC [21] power conversion and AC/DC conversion [22]. The ZSI can be used to buck or boost the input voltage without any need of a step up or DC to DC Switching converter. The SVPWM control strategy used to control the inverter bridge (six power transistor) is sufficient to achieve the desired output voltage. In this chapter the ZSI configuration is described in detail using the ZSI equivalent circuit. In addition, details about boosting a DC link voltage by utilizing the L-C impedance components is given, the usage of SVPWM is described and a simulation result model for the ZSI is presented and evaluated.

Using the ZSI, it is possible to

- produce the output voltage even greater than the input voltage,
- reduce the voltage and current harmonic so as to improve the power factor,
- extend ride-through during voltage sag without the need of adding any circuit.

3.2 The Z-Source Inverter

The configuration of three phase ZSI is demonstrated in Fig. 19. As described in [24], the Z-source inverter consists of two identical capacitors and two inverter which are connected in X-shape and composed to form a unique impedance to provide a coupling between the DC source input and the main inverter bridge circuit. Also, this impedance network avoids short circuit (destroying the DC input source) when the devices are in shoot-through operation mode by the diode which blocks a reverse current and protects the input DC source. The three phase ZSI has an additional parameter with the name

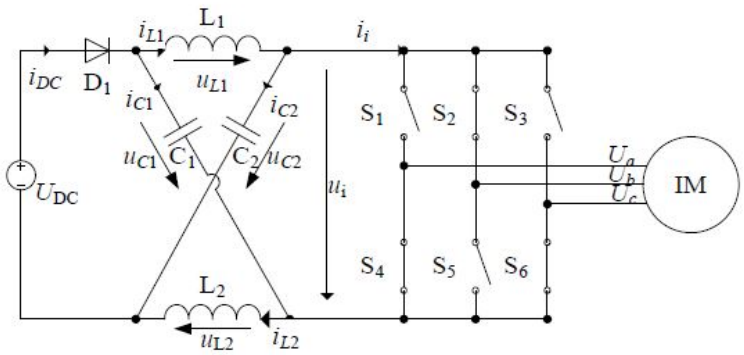

Figure 19: The ZSI with AC motor

Boost Factor (B) which is computed as

$$V_{out} = B \cdot M \cdot U_{DC}/2 \tag{3.1}$$

Here, V_{out} is the peak value of the AC output phase voltage, B is the boost factor, M is the modulation index, U_{DC} is the DC input voltage.

If we replace $B \cdot M$ with G, then can rewrite the equation by

$$V_{out} = G \cdot U_{DC}/2 \tag{3.2}$$

with the inverter gain G.

The boost factor can be evaluated depending on the shoot-through time T_{sh} and the switching time T_s as

$$B = \frac{1}{1 - 2 \cdot T_{sh}/T_s} \tag{3.3}$$

Using the shoot-through ratio $D_o = T_{sh}/T_s$, we get

$$B = \frac{1}{1 - 2 \cdot D_o} \tag{3.4}$$

One of the main differences between the ZSI and traditional inverters is that the ZSI has 9 permissible switching states: six active states, two zero states and one additional state called shoot-through state. A traditional voltage source inverter only has 8 states: six active states and two zero states.

3.3 Z-Source Inverter Operation

The ZSI with AC motor as shown in Fig. 19 can be divided into four main parts: the input DC voltage which is represented by a photovoltaic (PV) panel U_{DC} and the diode (D1) to avoid the short circuit during the shoot through; The X-shape symmetrical Z-source impedance, $C_1 = C_2$ and $L_1 = L_2$; the three phase inverter (six transistor power switch); the phase induction motor as a load .

The operation principle and control of the ZSI has been itemized in [9]. The outline of the ZSI operation modes are:

- Mode(1): In this mode, the inverter is operating in one of six active states while the diode (D1) is conducting. In this case the inverter bridge behaves as a current source as shown in Fig. 20 and the capacitor voltage $U_{c1} = U_{c2} = U_c$. Also, the inductor voltage fulfills $U_{L1} = U_{L2} = U_L$. Due to the symmetrical impedance network, the current and voltage relationships in this mode are

$$U_L = U_{DC} - U_c \tag{3.5}$$

$$U_i = 2 \cdot U_c - U_{DC} \tag{3.6}$$

$$i_{DC} = i_L + i_c \tag{3.7}$$

$$i_i = i_L - i_c \tag{3.8}$$

$$i_{DC} = 2 \cdot i_L - i_i \tag{3.9}$$

- Mode(2): In this mode the inverter bridge operate in one zero state and the in-

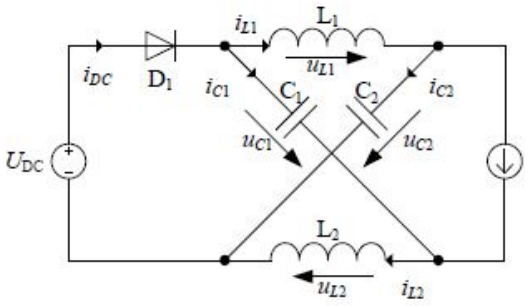

Figure 20: Operation of ZSI mode1

verter bridge operates as an open circuit. The voltage relationship is still the same as in mode(1), whereas the current relationship is modified to

$$i_{L1} = i_{L2} = i_{C1} = i_{C2} = i_{DC}/2 \tag{3.10}$$

- Mode(3): In this shoot-through mode, the diode in reverse biased because the sum of the voltage of the capacitor is higher than the input voltage. In this mode the inverter bridge of the ZSI operates in shoot through which is achievable by one phase, two phase legs or three phase legs. Fig. 21 and 22 display this situation. The current and voltage relationships in this mode are

$$U_L = U_C \tag{3.11}$$

$$U_i = 0 \tag{3.12}$$

$$i_{DC} = 0 \tag{3.13}$$

$$i_{L1} = -i_{C1} \tag{3.14}$$

$$i_{L2} = -i_{C2} \tag{3.15}$$

The shoot-through time T_{sh} depends on B and can be determined by.

$$T_{sh} = \frac{(B-1)\cdot T_s}{2\cdot B} \tag{3.16}$$

To determine the Z-source network impedance, the capacitor and inductor values must be defined. The parameters are listed in Table 2. The maximum output power P_{Omax} is related to the motor design. The switch frequency (FS) is one of the important parameters and it is necessary to determine the other parameters.

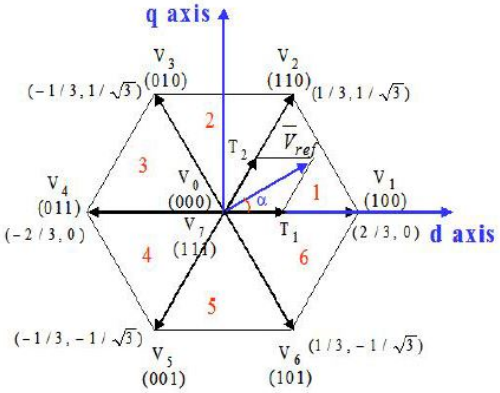

Figure 21: ZSI Mode3

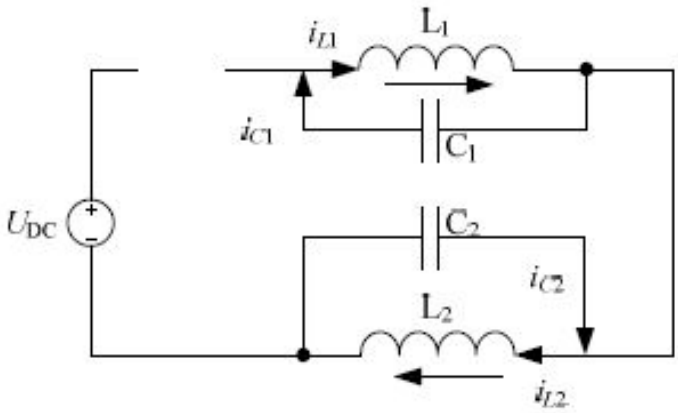

Figure 22: Operation of ZSI mode3

The Z-source components C, L, and the shoot-through duty cycle d_s are

$$d_s = \frac{V_o + V_{loss} - V_i}{2 \cdot (V_o + V_{loss}) - V_i} \tag{3.17}$$

$$I_o = P_{Omax}/V_o \tag{3.18}$$

$$I_L = (1 - \frac{d_s}{1 - 2d_s}) \cdot I_o \tag{3.19}$$

$$D_o = 1 - d_s \tag{3.20}$$

$$V_{DC} = V_o + V_{loss}/D_o \tag{3.21}$$

$$C = I_L d_s T_s / \Delta V_c \tag{3.22}$$

$$L \geq (1 - 2d_s) d_s T_s R_o \tag{3.23}$$

$$\tag{3.24}$$

D_o is the maximum duty cycle, I_o is the output current, V_{DC} is the DC link voltage and V_{loss} describes the switch and conduction losses of the wiring.

Table 2: Design Parameters of The Z-Source

Parameter	Symbol	Unit
Max.Output Power	P_{Omax}	W
Min.Output Power	P_{Omin}	W
Max.Output Voltage	V_{Omax}	V_{RMS}
Min.Output Voltage	V_{Omin}	V_{RMS}
Min.input voltage	V_{min}	V_{volt}
Operation Frequency	F_s	KHZ
Capacitor Ripple Voltage	ΔVC	m_V
Inductor Ripple Current	ΔIL	m_A

3.4 Space Vector Pulse With Modulation Implementation (SVPWM)

In this research, SVPWM is chosen to implement the Z-source inverter in order to get less harmonic distortion in the output voltage for more efficiency. For the ZSI which is shown in the Fig. 20, there are fifteen possible on-off configurations for the six power transistor switches which consists of the inverter bridge. As is listed in Table 3, there are six active states or non-zero states (V1 to V6), two non active state or zero state (V0 and V7). In these two cases, the ZSI operates in Mode1 and Mode2 (such as a traditional VSI) [25]. For the seven shoot-through states from V_{sh1} to V_{sh7}, the ZSI operates in Mode3.

Table 3: Switching States and Output Voltage of Three Phase ZSI

	S_a	S'_a	S_b	S'_b	S_c	S'_c	V_d	V_q
V_0	0	1	0	1	0	1	0	0
V_1	0	1	0	1	1	0	$-\sqrt{6}/6V_{dc}$	$-\sqrt{2}/2V_{dc}$
V_2	0	1	1	0	0	1	$-\sqrt{6}/6V_{dc}$	$\sqrt{2}/2V_{dc}$
V_3	0	1	1	0	1	0	$-\sqrt{6}/3V_{dc}$	0
V_4	1	0	0	1	0	1	$\sqrt{6}/3V_{dc}$	0
V_5	1	0	0	1	1	0	$\sqrt{6}/6V_{dc}$	$-\sqrt{2}/2V_{dc}$
V_6	1	0	1	0	0	1	$\sqrt{6}/6V_{dc}$	$\sqrt{2}/2V_{dc}$
V_7	1	0	1	0	1	0	0	0
V_{sh1}	1	1	b	b	c	c	0	0
V_{sh2}	a	a	1	1	c	c	0	0
V_{sh3}	a	a	b	b	1	1	0	0
V_{sh4}	1	1	1	1	c	c	0	0
V_{sh5}	1	1	b	b	1	1	0	0
V_{sh6}	a	a	1	1	1	1	0	0
V_{sh7}	1	1	1	1	1	1	0	0

As explained in Chapter 2, the realization of the SVPWM requires the dq transformation that transforms the three dimensional into a two dimensional vector in the dq coordinates:

$$\begin{bmatrix} V_d \\ V_q \end{bmatrix} = T_{abc-dq} \begin{bmatrix} V_a \\ V_b \\ V_c \end{bmatrix} = V_{dc} \cdot \begin{bmatrix} \sqrt{6}/3 & -1/\sqrt{6} & -1/\sqrt{6} \\ 0 & 1/\sqrt{2} & -1/\sqrt{2} \end{bmatrix} \begin{bmatrix} a \\ b \\ c \end{bmatrix} \tag{3.25}$$

There are eight possible switching vector on/off patterns for the three upper power transistor switches that feed the DC to AC power converter. As is shown in Fig. 14, these vectors divide the plane into six sectors and the angle between any neighboring active vectors is equal to 60 degrees.

To generate the same voltage as V_{ref} without boost voltage we need to determine the three switching time durations ($T1, T2, T0$) for each sector by using the most adjacent two voltage vectors and the constant switching period (T_z). The details for computing the time durations for each sector are as follows.

A. Sector 1: $0 \leq \alpha \leq \pi/3$. We get the following equations

$$\int V_{ref} = \int V1dt + \int V2dt + \int V0dt \tag{3.26}$$

$$T_z \cdot V_{ref} = (T1 \cdot V1 + T2 \cdot V2) \tag{3.27}$$

$$a = 2 \cdot |V_{ref}|/V_{dc} \tag{3.28}$$

Therefore, the switching time interval can be determined by

$$T1 = 2/\sqrt{3} \cdot T_z \cdot a \cdot \sin(\pi/3 - \alpha) \tag{3.29}$$

$$T2 = 2/\sqrt{3} \cdot T_z \cdot a \cdot \sin(\alpha) \tag{3.30}$$

$$T0 = T_z - (T1 + T2) \tag{3.31}$$

B. Sector 2: $\pi/3 \leq \alpha \leq 2\pi/3$. We get the following equations

$$T2 = 2/\sqrt{3} \cdot T_z \cdot a \cdot \sin(2\pi/3 - \alpha) \tag{3.32}$$

$$T3 = 2/\sqrt{3} \cdot T_z \cdot a \cdot \sin(\alpha - \pi/3) \tag{3.33}$$

$$T0 = T_z + (T2 + T3) \tag{3.34}$$

C. Sector 3: $2\pi/3 \leq \alpha \leq \pi$. We get the following equations

$$T3 = 2/\sqrt{3} \cdot T_z \cdot a \cdot \sin(\pi - \alpha) \tag{3.35}$$

$$T4 = 2/\sqrt{3} \cdot T_z \cdot a \cdot \sin(\alpha - 2\pi/3) \tag{3.36}$$

$$T0 = T_z - (T3 + T4) \tag{3.37}$$

D. Sector 4: $\pi \leq \alpha \leq 4\pi/3$. We get the following equations

$$T4 = 2/\sqrt{3} \cdot T_z \cdot a \cdot \sin(4\pi/3 - \alpha) \tag{3.38}$$

$$T5 = 2/\sqrt{3} \cdot T_z \cdot a \cdot \sin(\alpha - \pi) \tag{3.39}$$

$$T0 = T_z - (T4 + T5) \tag{3.40}$$

E. Sector 5: $4\pi/3 \leq \alpha \leq 5\pi/3$. We get the following equations

$$T5 = 2/\sqrt{3} \cdot T_z \cdot a \cdot \sin(5\pi/3 - \alpha) \tag{3.41}$$

$$T6 = 2/\sqrt{3} \cdot T_z \cdot a \cdot \sin(\alpha - 4\pi/3) \tag{3.42}$$

$$T0 = T_z - (T5 + T6) \tag{3.43}$$

F. Sector 6: $5\pi/3 \leq \alpha \leq 2\pi$. We get the following equations

$$T6 = 2/\sqrt{3} \cdot T_z \cdot a \cdot \sin(2\pi - \alpha) \tag{3.44}$$

$$T1 = 2/\sqrt{3} \cdot T_z \cdot a \cdot \sin(\alpha - 5\pi/3) \tag{3.45}$$

$$T0 = T_z - (T6 + T1) \tag{3.46}$$

The state pulse pattern of the space vector modulation (SVM) for 3-phase inverters begins with the non-active state (V_{000}) that forces all the upper transistor switches to becomes open. This state is followed by two active states and the state pulse pattern ends with another non-active state (V_{111}). All upper transistor switches are forced to be closed. This sequence repeats in reverse order after half of the switching period $T_s/2$. Using the symmetrical pulse pattern, the two non-active states are divided equally on both ends of the active state as illustrated in Table 4.

Table 4: Switch Time Calculation at Each Sector

Sector	Upper Switches (S1,S3,S5)	Lower Switches (S4,S6,S2)
1	$S_1 = T_1 + T_2 + T_0/2$ $S_3 = T_2 + T_0/2$ $S_5 = T_0/2$	$S_4 = T_0/2$ $S_6 = T_1 + T_0/2$ $S_2 = T_1 + T_2 + T_o/2$
2	$S_1 = T_1 + T_0/2$ $S_3 = T_1 + T_2 + T_0/2$ $S_5 = T_0/2$	$S_4 = T_2 + T_0/2$ $S_6 = T_0/2$ $S_2 = T_1 + T_2 + T0/2$
3	$S_1 = T_0/2$ $S_3 = T_1 + T_2 + T_0/2$ $S_5 = T_2 + T_0/2$	$S_4 = T_1 + T_2 + T_0/2$ $S_6 = T_0/2$ $S_4 = T_1 + T_0/2$
4	$S_1 = T_0/2$ $S_3 = T_1 + T_0/2$ $S_5 = T_1 + T_2 + T_0/2$	$S_4 = T_1 + T_2 + T_0/2$ $S_6 = T_2 + T_0/2$ $S_2 = T_0/2$
5	$S_1 = T_2 + T_0/2$ $S_3 = T_0/2$ $S_5 = T_1 + T_2 + T_0/2$	$S_4 = T_1 + T_0/2$ $S_6 = T_1 + T_2 + T_0/2$ $S_4 = T_0/2$
6	$S_1 = T_1 + T_2 + T_0/2$ $S_3 = T_0/2$ $S_5 = T_1 + T_0/2$	$S_4 = T_0/2$ $S_6 = T_1 + T_2 + T_0/2$ $S_2 = T_2 + T_0/2$

3.5 Simulation Results

In order to demonstrate the proposed model and control techniques, a simulation model is realized using Matlab/Simulink with a nonlinear load represented by an induction motor with 4KW. We assume that the output voltage of the PV module is 220 V and the system parameters are given in Table 5. Fig. 23 shows the three phase output current of the ZSI (without boost). Fig. 24, Fig. 25 and Fig. 26, show the phase(A), phase(B) and phase(C) output voltage

Table 5: System Parameters

Parameter	**Value**	**units**
High performance ZSI Parameters		
Inductance	250	micro H
capacitance	350	micro F
Switching frequency	2000	HZ
Input Voltage	400	volt
Induction motor parameter		
output power	4	KW
line voltage	220	volt
stator resistance R_s	1.4	ohm
rotor resistance R_r	1.39	ohm
stator inductance L_Ls	0.00058	H
rotor inductance L_Lr	0.0058	H
Mutual inductance L_m	0.1722	H

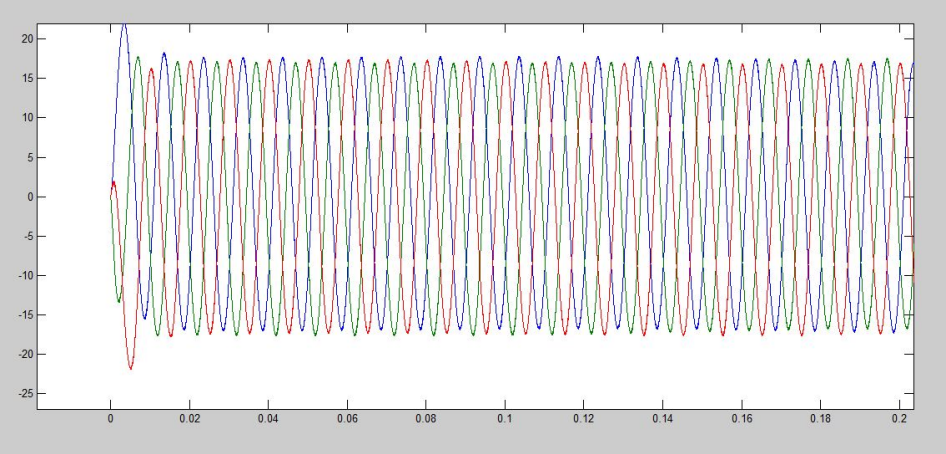

Figure 23: Three phase output current

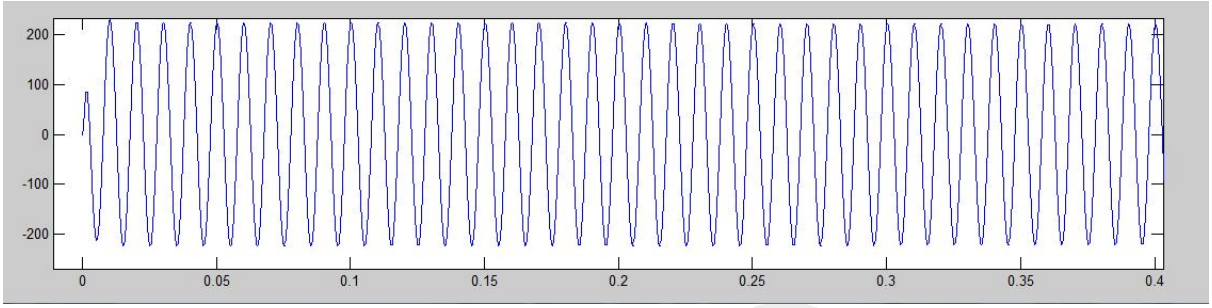

Figure 24: Phase A AC voltage without boost

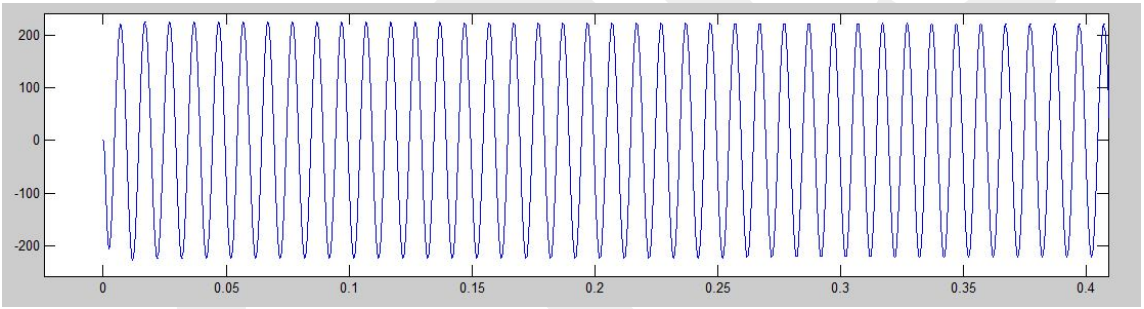

Figure 25: Phase B AC voltage without boost

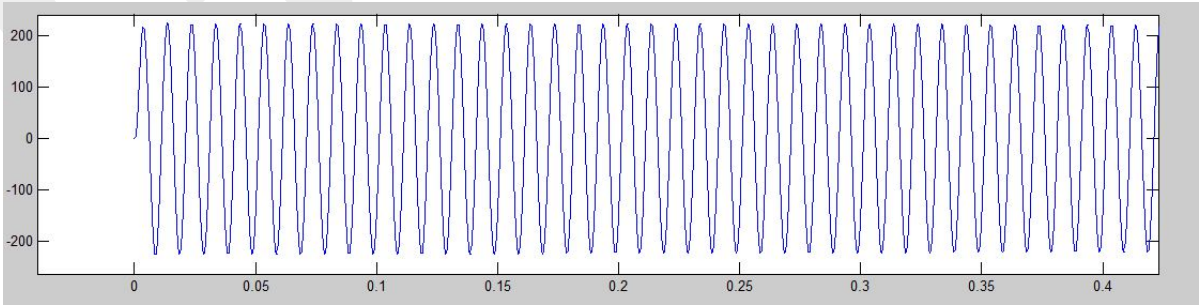

Figure 26: Phase C AC voltage without boost

In this configuration, the ZSI operates as the traditional VSI and the ZSI switching states only comprise the first seven states (V0 to V7). Consider Fig. 27, Fig. 28. which show the switch state for switch 1, switch 4. In these figures, we can not see switch 1 and switch 4 on at the same time. The same holds also for switch 3 and switch 6 also for switch 5 and switch 2.

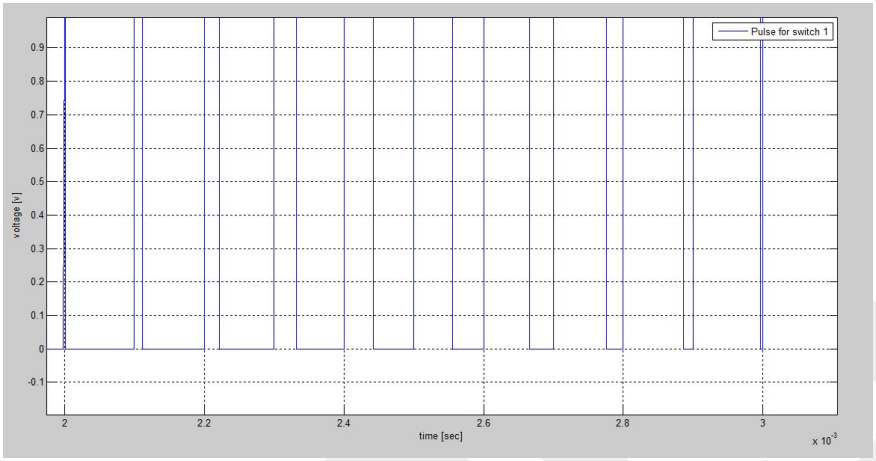

Figure 27: Switch 1 state

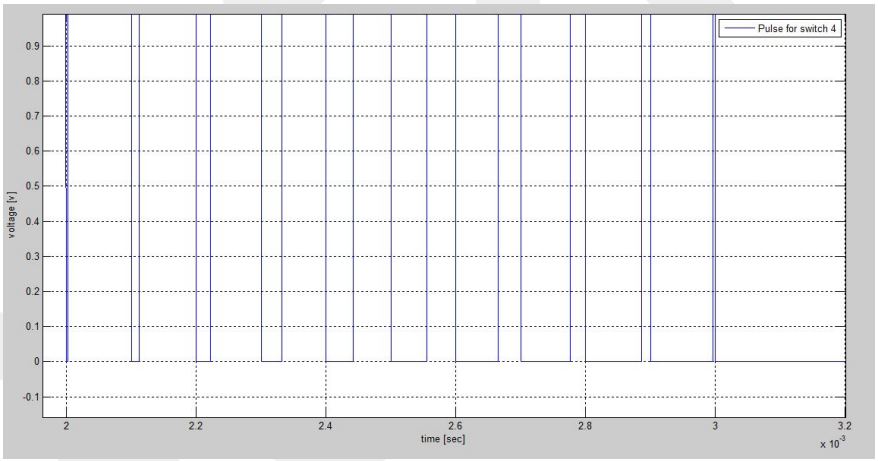

Figure 28: Switch 4 state

3.6 Z-Source Inverter With Boost

In the previous section it was noted that the ZSI can be operated as a traditional voltage source inverter (VSI). This section explains the possible voltage boost of the ZSI based on [26, 27]. For the implementation of the ZSI with shoot-through states, the traditional SVPWM technique must be modified. In order to boost the DC- Link voltage of the ZSI and to produce the sinusoidal AC output voltage, a new time duration T is added to the switching times $T1$, $T2$ and $T0$ of the conventional SVPWM. Hereby, the shoot-through time T_a divided between the three legs such that $T_a = 3 \cdot T$. The switching times of the modified space vector pulse width modulation (MSVPWM) for the upper power transistor switches and lower power transistor switches in a 3-phase inverter is summarized in Table 6.

Table 6: Switch Time Calculation at Each Sector With Boost

Sector	Upper Switches (S1,S3,S5)	Lower Switches (S4,S6,S2)
1	$S_1 = T_1 + T_2 + T_0/2 + T$ $S_3 = T_2 + T_0/2$ $S_5 = T_0/2 - T$	$S_4 = T_0/2$ $S_6 = T_1 + T_0/2 + T$ $S_2 = T_1 + T_2 + T_o/2 + 2T$
2	$S_1 = T_1 + T_0/2$ $S_3 = T_1 + T_2 + T_0/2 + T$ $S_5 = T_0/2 - T$	$S_4 = T_2 + T_0/2 + T$ $S_6 = T_0/2$ $S_2 = T_1 + T_2 + T0/2 + 2T$
3	$S_1 = T_0/2 - T$ $S_3 = T_1 + T_2 + T_0/2 + T$ $S_5 = T_2 + T_0/2$	$S_4 = T_1 + T_2 + T_0/2 + 2T$ $S_6 = T_0/2$ $S_4 = T_1 + T_0/2 + T$
4	$S_1 = T_0/2 - T$ $S_3 = T_1 + T_0/2$ $S_5 = T_1 + T_2 + T_0/2 + T$	$S_4 = T_1 + T_2 + T_0/2 + 2T$ $S_6 = T_2 + T_0/2 + T$ $S_2 = T_0/2$
5	$S_1 = T_2 + T_0/2$ $S_3 = T_0/2 - T$ $S_5 = T_1 + T_2 + T_0/2 + T$	$S_4 = T_1 + T_0/2 + T$ $S_6 = T_1 + T_2 + T_0/2 + 2T$ $S_4 = T_0/2$
6	$S_1 = T_1 + T_2 + T_0/2 + T$ $S_3 = T_0/2 - T$ $S_5 = T_1 + T_0/2$	$S_4 = T_0/2$ $S_6 = T_1 + T_2 + T_0/2 + 2T$ $S_2 = T_2 + T_0/2 + T$

The traditional and modified switching patterns for the ZSI in the six sectors is compared in Fig. 29 to 34.

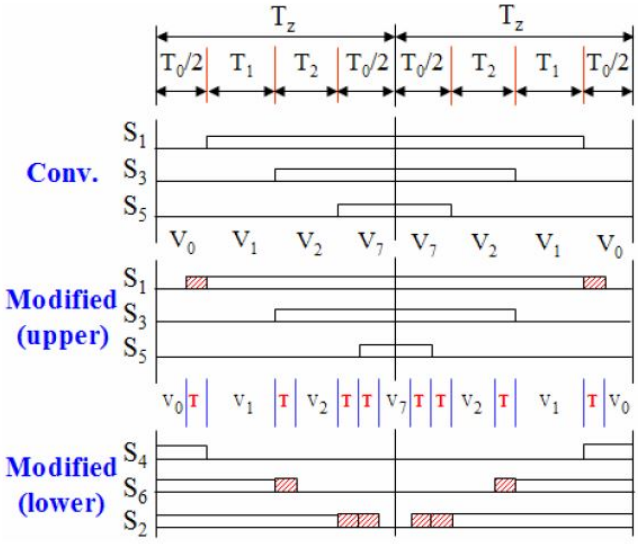

Figure 29: MSVPWM sector 1

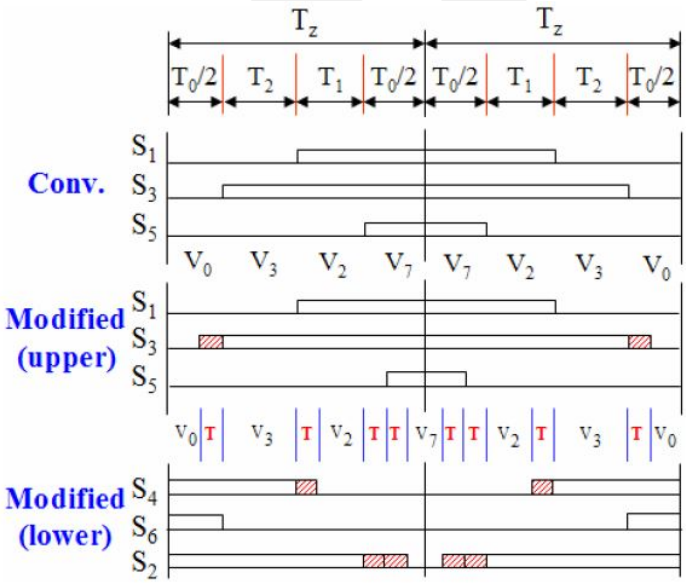

Figure 30: MSVPWM sector 2

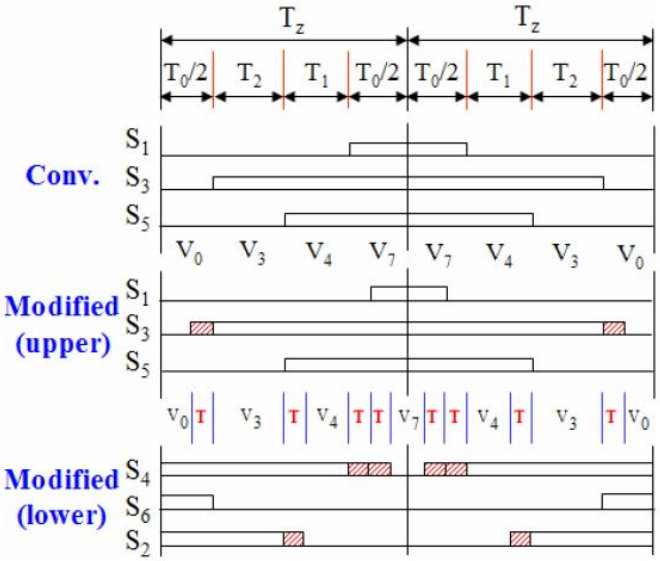

Figure 31: MSVPWM sector 3

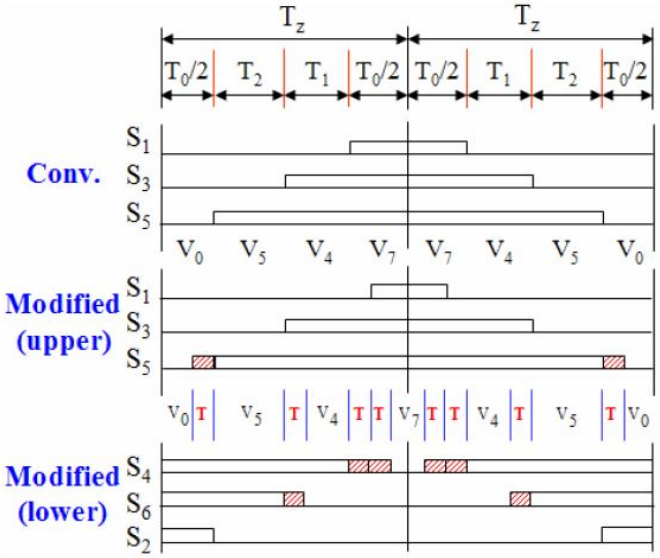

Figure 32: MSVPWM sector 4

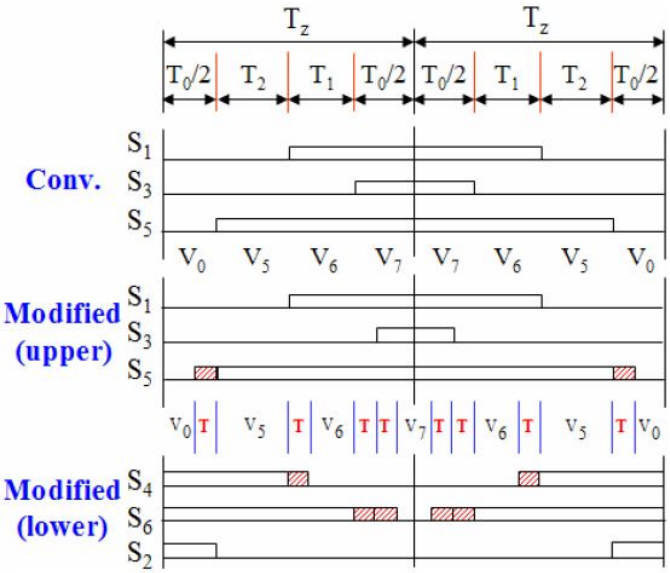

Figure 33: MSVPWM sector 5

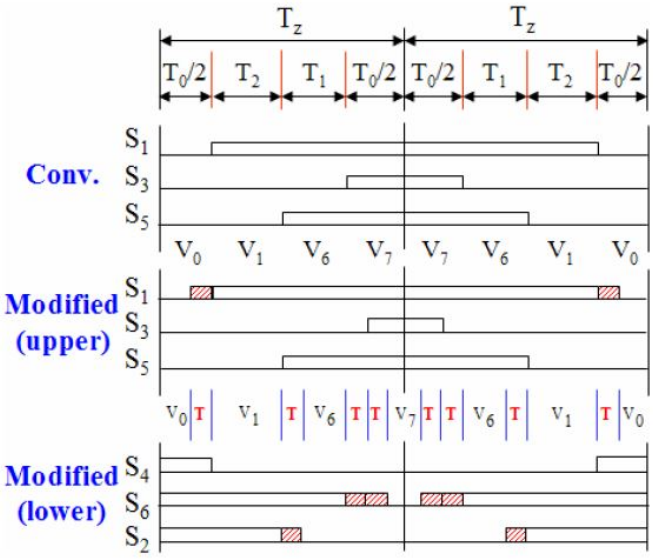

Figure 34: MSVPWM sector 6

Next, the relevant switching times are computed for the ZSI with voltage boost. First, the desired voltage gain is evaluated as

$$G = \frac{V_o}{V_i/2} \tag{3.47}$$

with the DC input voltage V_i and the phase output peak voltage V_o. We recall that V_o is related to the 3-phase line voltage by

$$V_{line} = \sqrt{3} \cdot V_o. \tag{3.48}$$

Using

$$M = \frac{\pi G}{3\sqrt{3}G - \pi}, \tag{3.49}$$

the modulation index M can be determined from G. Then, it follows for the D duty ratio that related with M

$$D = 1 - M \tag{3.50}$$

the boost factor B is determined from DC link voltage and V_i

$$B = \frac{V_{DC}}{V_i} \tag{3.51}$$

leading to the shoot-through time

$$T_{sh} = \frac{(B-1) \cdot T_s}{2 \cdot B} \tag{3.52}$$

Finally, T_{sh} is divided in to three equal time intervals $T = T_{sh}/3$.

Including the shoot-through state, we can rewrite the zero time durations in each sector as follows

A. Sector 1

$$T0 + T_a = T_z[1 - \sqrt{3}/2 \cdot M \cdot \cos(\alpha - \pi/6)] \tag{3.53}$$

B. Sector 2

$$T0 + T_a = T_z[1 - \sqrt{3}/2 \cdot M \cdot \sin\alpha] \tag{3.54}$$

C. Sector 3

$$T0 + T_a = T_z[1 + \sqrt{3}/2 \cdot M \cdot \cos(\alpha + \pi/6)] \tag{3.55}$$

D. Sector 4

$$To + T_a = T_z[1 + \sqrt{3}/2 \cdot M \cdot \cos(\alpha - \pi/6)] \tag{3.56}$$

E. Sector 5

$$T0 + T_a = T_z[1 + \sqrt{3}/2 \cdot M \cdot \sin\alpha] \tag{3.57}$$

F. Sector 6

$$T0 + T_a = T_z[1 + \sqrt{3}/2 \cdot M \cdot \cos(\alpha + \pi/6)] \tag{3.58}$$

Here, we use $T_z = T_a + T_b$ with the switching period T_z, the total duration of the non-shoot-through state T_b and the shoot-through duration T_a The DC-link voltage and the inverter output voltage can be controlled by setting T_a. The zero vector duration $T0/2$ which is determined by the modulation index M limits the maximum available shoot through interval T_a to boost the DC link voltage and the output AC voltage of inverter.

3.7 Simulation Results With Voltage Boost

3.7.1 Simulator in Simulink

We realize a simulation model of the ZSI with voltage boost in Simulink. The block diagram is shown in Fig. 35. The input is a voltage reference signal that is decomposed into its magnitude and phase angle. Then, the switching times with shoot-through states are evaluated. Based on these switching times, the pulses of the SVPWM are determined and fed to an IGBT (insulated-gate bipolar transistor) inverter that is connected to the ZSI network. The generated three-phase output voltage is used to drive an AC motor.

Examples of the switch states with boost are given in Fig. 36 and 37.

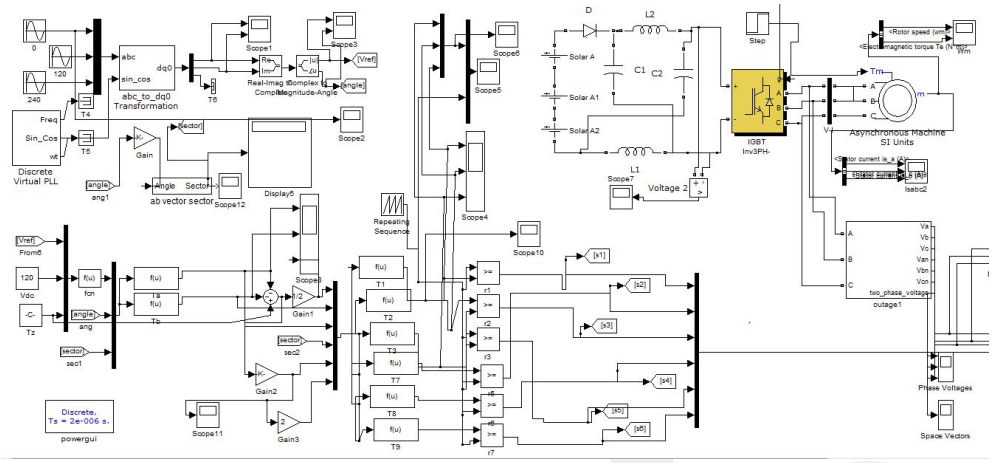

Figure 35: Simulation ZSI block diagram with boost

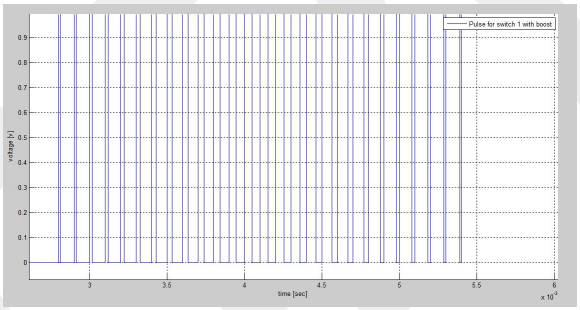

Figure 36: State of switch1 with boost

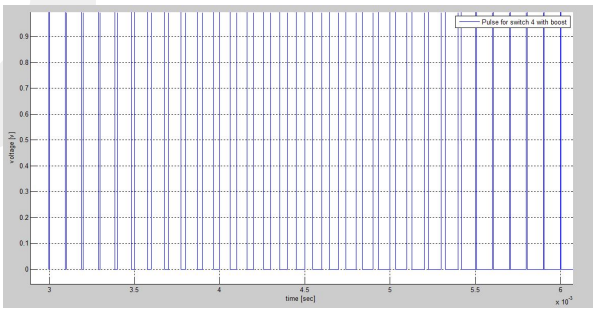

Figure 37: State of switch4 with boost

3.7.2 Simulation Results

Next, the simulator in Section 3.7.1 is used to evaluate the functionality of the ZSI with voltage boost. The ZSI consists of $L1 = L2 = L = 250MH$ and $C1 = C2 = C = 300MF$. The output of the PV modules is represented by the input DC voltage of 120V and the switching frequency $f_s = 2KHz$ is chosen. The AC motor as a load is connected to the output of inverter. The simulation results are shown in, Fig. 38 to 41.

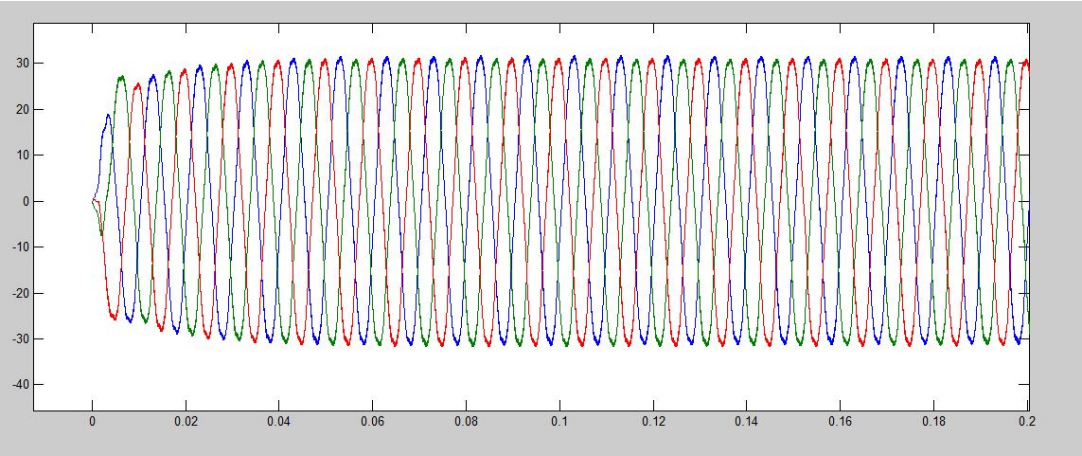

Figure 38: Three phase current with boost

It can be seen from Fig. 35 that a three-phase current with 120 degrees phase difference is generated. In addition, Fig. 39 to 41 show that a three-phase voltage with the desired frequency and a voltage boost to 400 V is obtained.

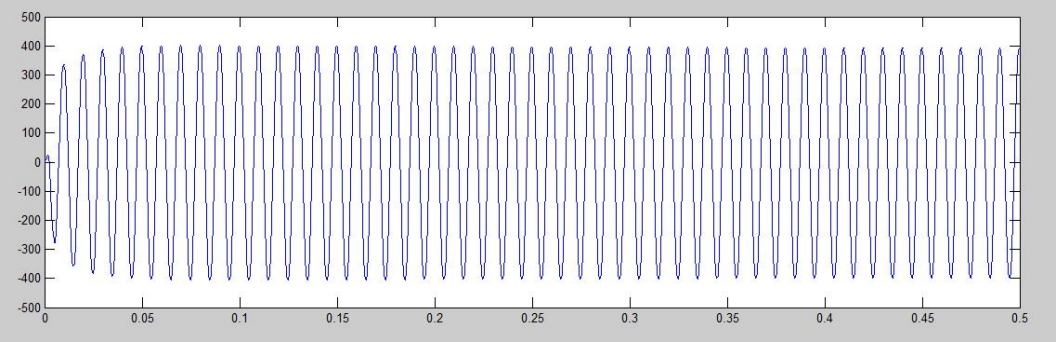

Figure 39: Phase A voltage with boost

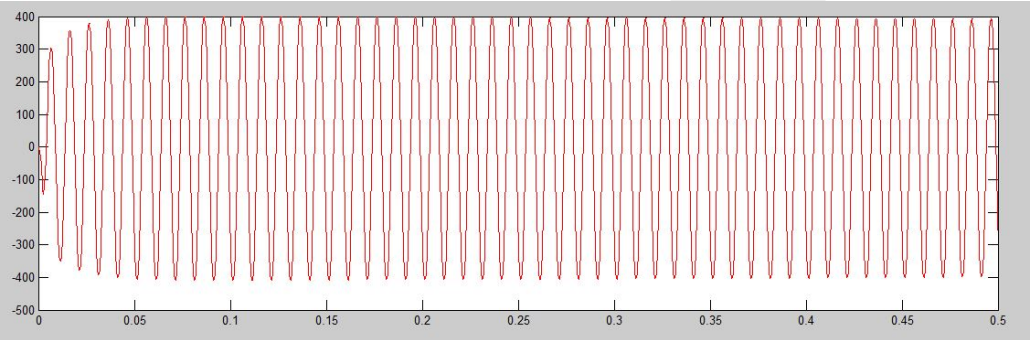

Figure 40: Phase B voltage with boost

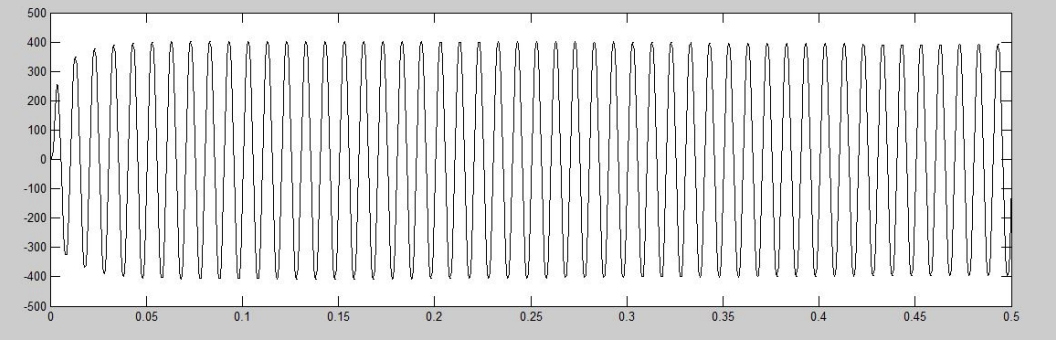

Figure 41: Phase C voltage with boost

CHAPTER 4

AC MOTOR CONTROL USING THE Z-SOURCE

4.1 V/F Control

In order to control the AC motor speed, we apply the V/f (voltage per frequency) scalar control technique [28, 29]. This technique is used for induction motor drives with inverters in a large number of industrial application because of the low cost and implementation complexity. In this method, the speed of the induction motor is controlled by the adjustable magnitude of the stator voltage and frequency. The main effect is that the air gap flux is always maintained at the required value in the steady state (scalar control focuses on the steady-state behavior).

The working principle of V/f scalar control can be understood when looking at the simplified version of the steady-state electrical equivalent circuit as shown in Fig. 42. R_s represents the stator resistance which is assumed to be equal to zero, L_{ls} is the

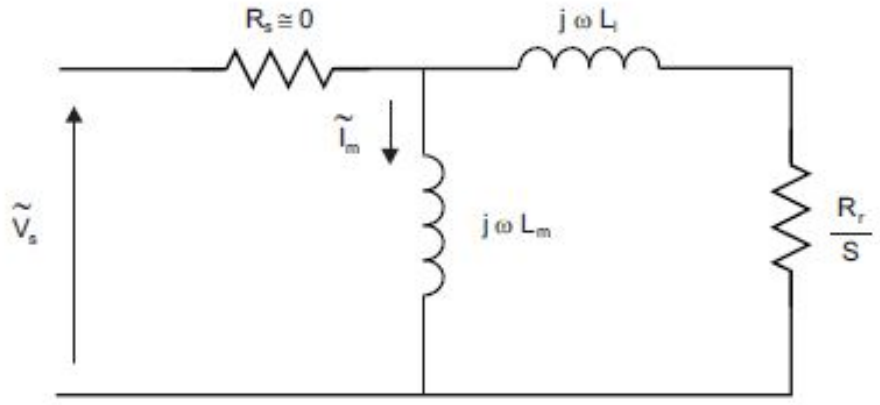

Figure 42: Equivalent circuit of induction motor

stator leakage inductance which is embedded into the (referred to stator) rotor leakage inductance ,L_{lr} represents the amount of air gap flux, L_l is the total leakage inductance

equal to

$$L_l = L_{ls} + L_{lr} \tag{4.1}$$

The magnetizing current that generates the air gap flux is almost equal to the stator voltage to frequency ratio.

$$I_m = \frac{V_s}{X_m} \tag{4.2}$$

$$I_m = \frac{V_s}{2\pi f_s L_m} \tag{4.3}$$

I_m is the magnetizing phase current, V_s is the supply phase voltage, f is the supply frequency and X_m is the (constant) magnetizing inductance.

When the three phase induction motor operates in the linear magnetic region, the above equation can be shown in terms of magnitude as

$$I_m = \frac{\Lambda_m}{L_m} = \frac{V_s}{2\pi f_s L_m} \tag{4.4}$$

Hereby, Λ_m represent the stator flux.

From the last equation it follows that the flux remains constant if the relationship V/F remains constant. That is, the torque becomes independent of the frequency supply. Hence, it is desired at different speeds to keep the ratio V_s/F constant. This means that the stator voltage must increase proportionally to the frequency so as to keep V_s/F constant. However, the frequency (or synchronous speed) can not slip out of the actual speed depending on the motor load. If there is no load, the slip is very small and the motor speed is nearly equal to the synchronous speed. Then, the open loop V/F control will achieve the desired speed, while the V/F system cannot fully control the speed if a load is applied on the motor. The slip corrections can be added to the system with measurement of the speed. Fig. 43, shows the closed-loop V/F control system with speed sensor measurement.

Commonly the V/F ratio depends on the rated values of these variables. As shown in Fig. 43, there are three speed ranges in the V/F control system which are listed below.

- Region $0 - f_c$ Hz: In this region there is non-negligible voltage drop across the stator resistance that must be compensated by increasing the stator voltage. Here, the V/F profile is not in linear state. The cutoff frequency f_c and the stator

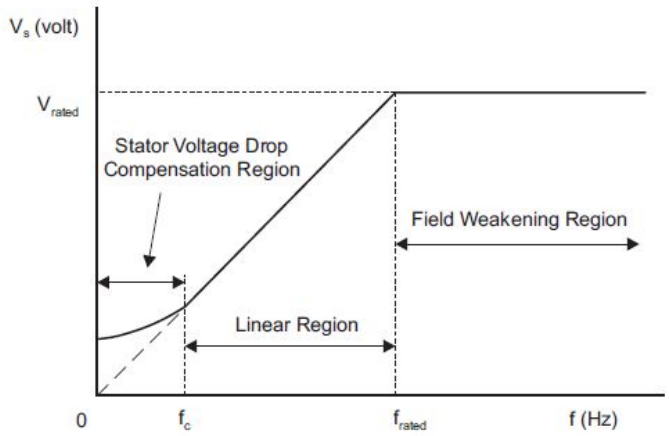

Figure 43: Stator voltage with frequency by using V/F control

voltage can be computed from the steady-state equivalent circuit with $R_s \neq 0$.

- Region $f_c - f_{rated}$ Hz: Here, the V/F profile is linear, whereby the slope represents the amount of air gap flux.
- Region above f_{rated} Hz: At higher frequencies is not possible to keep the V/F ratio constant. Since the stator voltage is limited to the rated value, the air gap flux is reduced which is decreases the torque.

If the stator flux is constant, the torque depends only on the slip speed as shown in Fig. 44. With the constant V/F ratio, the torque and speed of a three phase AC induction motor can be controlled by regulating the slip speed [30],[31].

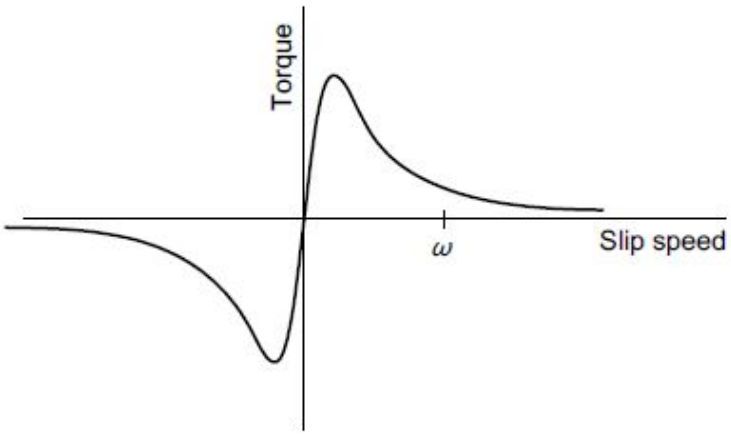

Figure 44: The torque and slip speed for induction motor by using V/F

4.2 Design Parameters for the ZSI

In order to design the ZSI, several input parameters are taken into account in order to compute the relevant design parameters. Since this chapter focuses on the ZSI design for different experimental settings, the most important design parameters are summarized. As input parameters, the minimum input voltage V_{min}, the desired output voltage V_o, the voltage loss V_{loss}, the maximal output power P_{Omax} and the output current I_o. Using these parameters, the shoot-through duty cycle ds, the maximum duty cycle D, the DC link voltage V_{DC}, the capacitor value C and the inductor value L of the ZSI. The following equations show how to determine these parameters.

$$d_s = \frac{V_o + V_{loss} - V_{min}}{2 \cdot (V_o + V_{loss}) - V_{min}} \tag{4.5}$$

$$D = 1 - d_s \tag{4.6}$$

$$V_{DC} = V_o + V_{loss}/D \tag{4.7}$$

$$I_o = P_{Omax}/V_o \tag{4.8}$$

$$I_L = (1 - d_s/1 - 2d_s) \cdot I_o \tag{4.9}$$

$$C = I_L d_s T_s / \Delta V_c \tag{4.10}$$

$$L \geq (1 - 2d_s) d_s T_s R_o \tag{4.11}$$

$$\tag{4.12}$$

To determine the shoot-through time we need to compute

$$G = \frac{V_o}{V_i/2} \tag{4.13}$$

using

$$V_{line} = \sqrt{3} \cdot V_o \tag{4.14}$$

$$M = \frac{\pi G}{3\sqrt{3}G - \pi}, \tag{4.15}$$

From the boost factor

$$B = \frac{V_{DC}}{V_i} \tag{4.16}$$

we get the shoot-through time

$$T_{sh} = \frac{(B-1)\cdot T_s}{2\cdot B} \tag{4.17}$$

4.3 Simulation Model

In order to apply the open loop V/F control technique for speed control experiments, a simulation model is prepared in Matlab/Simulink. It is based on the simulation model in Chapter 3, using the implemented SVPWM method with voltage boost. The reference voltage is generated from the desired frequency using the V/F relationship as described in Section 4.1. Fig. 45 shows the Simulink block diagram of open loop speed control.

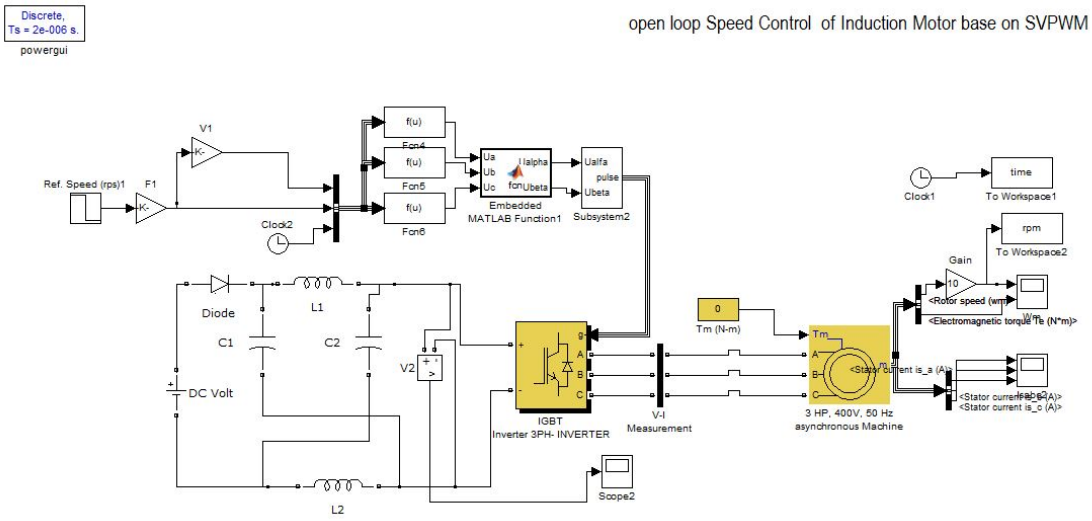

Figure 45: Simulation open loop operation of induction motor

4.4 Custom ZSI Designs for Different AC Motors

The summary of the ZSI design computations in Section 4.2 shows that it is possible to perform a custom ZSI design depending on the parameters of the respective AC motor. In this section, we perform two custom designs for two different AC motors. Hereby, we assume that the minimum input DC voltage is given by $V_{min} = 225$ V. The AC motor parameters and ZSI design parameters according to Section 4.2 are listed in Table 7.

Table 7: Custom Design Parameters for Two AC Motors

Parameter	Motor 1	Motor 2
nominal voltage	460 Volt	575 Volt
nominal motor speed	1750 rpm	1750 rpm
output powerP_o	3730 W	3730 W
inductor value L	0.850mH	1.1 mH
capacitor value C	19mF	22mF
boost factor(B)	2.1	2.2555
voltage gain(G)	3.338	4.1

In addition, we show reference step responses for different reference speeds of the AC motors. The result for motor 1 is shown in Fig. 46 and the result for motor 2 is shown in Fig. 47.

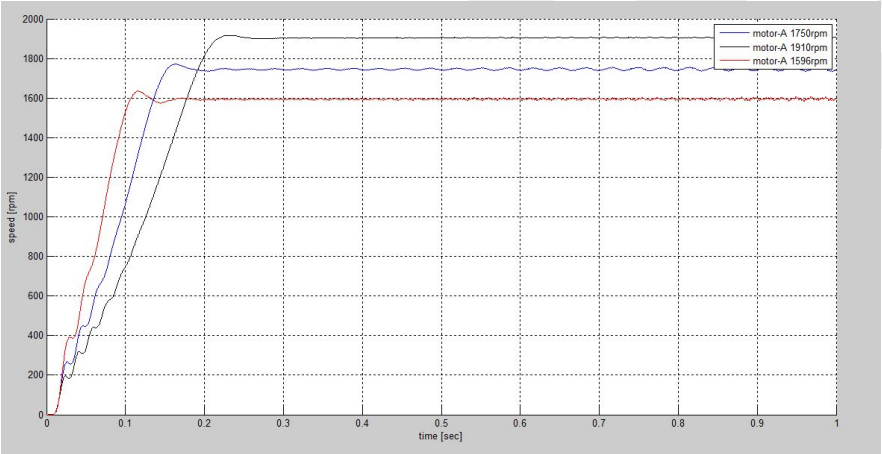

Figure 46: Custom ZSI design for motor 1

It can be seen from the figures that all desired speeds are reached. That is, the ZSI designs with voltage boost are suitable to provide the necessary DC link voltage for the speed control of both AC motors.

4.5 General ZSI Design to Support Different AC Motors

In this section, we investigate the usage of a single ZSI design for different AC motors. To this end, we consider the same AC motors as in Section 4.4. For the ZSI design, we again assume that the DC input voltage is 225 V. Nevertheless, since two different motors with different voltage levels of 460 V and 575 V, respectively, are used, we design the ZSI for the average voltage level.

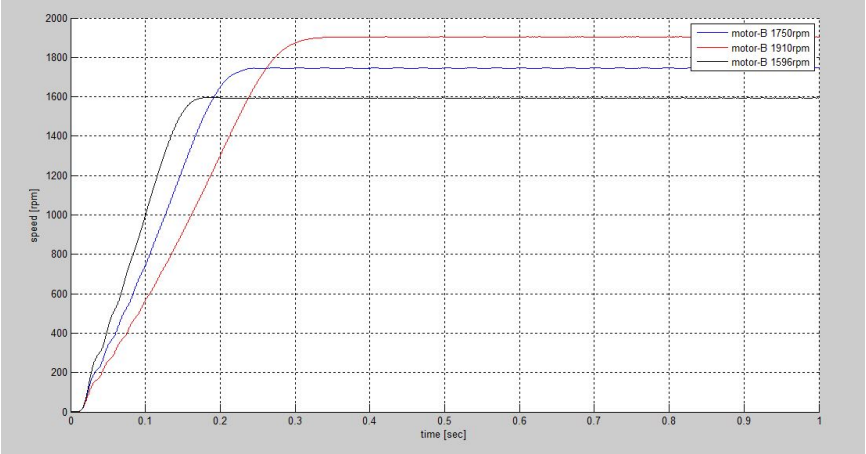

Figure 47: Custom ZSI design for motor 2

We now compare the reference step responses for the design in this section and the custom design in Section 4.4. Fig. 48 shows the comparison for motor 1 and Fig. 49 shows the comparison for motor 2.

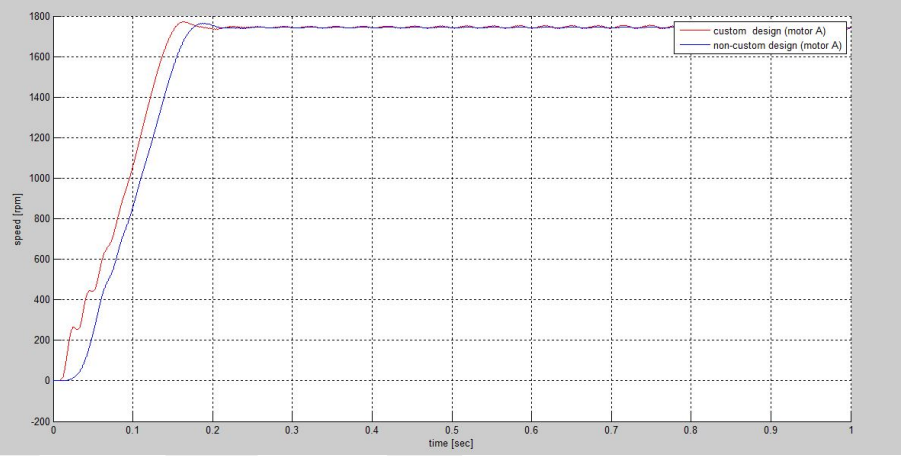

Figure 48: Comparison of custom and non-custom design for motor 1

It can be seen for both motors that the desired motor speed is reached. However, it can be noted that the output response is slightly slower in case of a non-custom design. That is, choosing non-custom parameters for the ZSI design leads to a suitable performance of the AC motor control with a very small degradation of the output response.

4.6 Dependency of System Response on Input Voltage

In this section, we investigate the effect of different input DC voltages on the output response of the AC motor. To this end, we focus on motor 1 in Section 4.4 and consider the DC input voltages 225 V, 300 V and 400 V. We use the custom ZSI hardware for

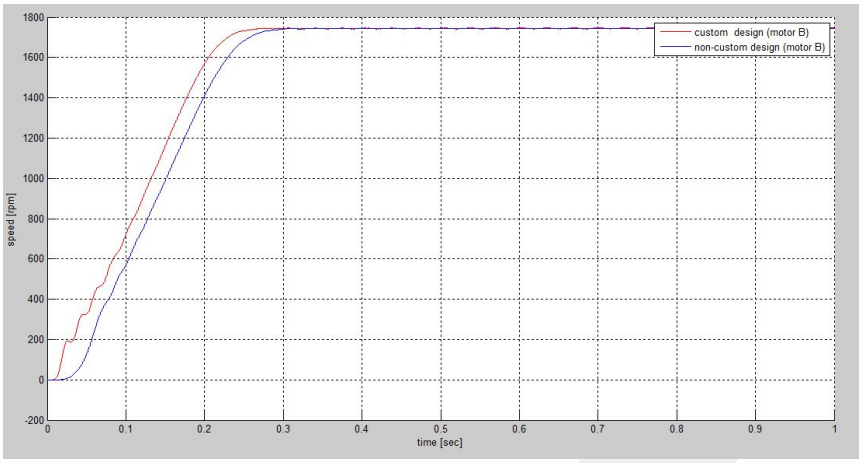

Figure 49: Comparison of custom and non-custom design for motor 2

motor 1 and the DC input voltage 225 V. Only the boost ratio is modified depending on the different DC input voltages. Fig. 50 show the reference step responses for the different DC input voltages.

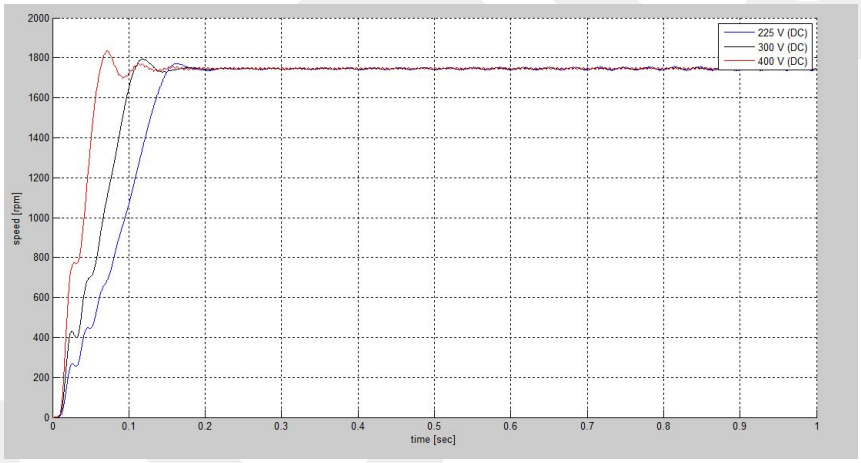

Figure 50: Dependency of output response on DC input voltage for motor1

It is readily observed that the ZSI is suitable for all considered DC input voltages. In addition, it has to be noted that a reduced DC input voltage potentially leads to a slightly slower output response.

4.7 Fluctuations in the DC Input Voltage

In this section, we investigate fluctuations of the DC input voltage that is supplied by the PV module. To this end, we replace the DC voltage source in the simulation by a controlled voltage source and perform a gradual increase of the DC input voltage. A comparison of the output response with and without DC input voltage fluctuation is

shown in Fig. 51.

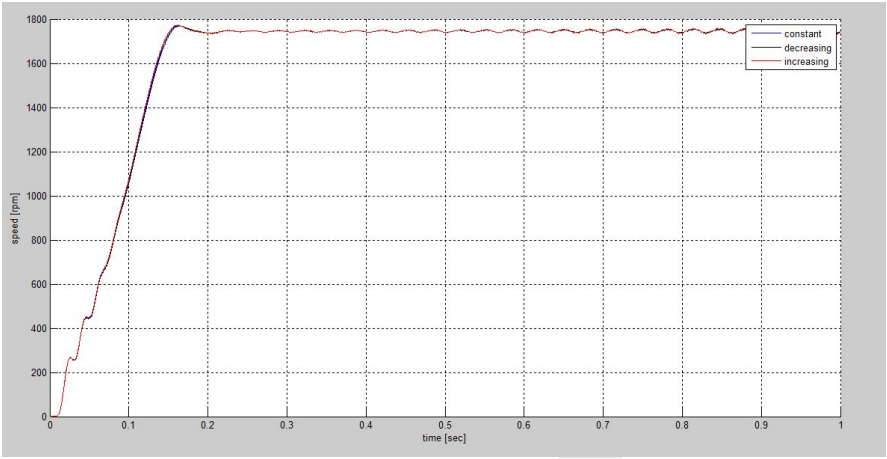

Figure 51: Dependency of output response on fluctuations in DC input voltage

It is readily observed that the fluctuations in the DC input voltage are negligible. This is one of the advantages of the ZSI in combination with SVPWM.

CHAPTER 5

CONCLUSION AND FUTURE WORK

The subject of this thesis is the AC motor control using the Z-source inverter (ZSI) with a DC input voltage from a photovoltaic (PV) module. Hereby, the important feature of the ZSI is the voltage boost of a potential low DC voltage of a PV module to the higher required voltage level of an AC motor. The thesis first develops the model equations of the ZSI and determines the relevant design parameters including the realization of voltage boost. In order to generate an AC output voltage, the idea of space vector pulse width modulation (SVPWM) is used. In the first part of the thesis, a simulation environment for the ZSI is developed in Simulink and different scenarios are evaluated. It is verified that the ZSI design computations match the results obtained by simulation.

The second part of the thesis focuses on the AC motor control using the ZSI. The V/f (voltage per frequency) control technique is employed in order to achieve the desired speed set-points of the AC motor. Different simulation experiments are employed in order to support the usability of the ZSI. First, an experiment with different AC motors and customized ZSI designs is conducted. It shows that a correctly designed ZSI successfully allows speed adaptations of the AC motor. In the second experiment, a single ZSI hardware is designed for different AC motors. This experiment shows that the same ZSI hardware can be suitable for AC motors with different characteristics by simply changing the boost ratio in software. The usage of different DC input voltages for the same ZSI hardware is studied in the third experiment. Here, it turns out that the same ZSI hardware can indeed be used with an appropriate change of the boost ratio. Nevertheless, the output responses of the AC motor speed slow down for smaller DC input voltages. In the last experiment, we show that fluctuations of the DC input voltage only have a small effect on the output response of the AC motor.

In summary, the thesis provides a comprehensive design framework for ZSIs which are used for the AC motor control with an extensive simulation study. In future work, several improvements can be considered:

- It is possible to apply the same idea to different input DC voltage sources such as fuel cells,
- It is possible to extend the considered system by feedback control,
- A hardware implementation of the designed VSIs and the related hardware experiments can be performed in future work.

REFERENCES

1. **Kazmierkowski M. P., Malesani L., (1998),** *"Current Control Techniques for Three Phase Voltage-Source PWM Converters: a Survey"*, IEEE Transaction on Industrial Electronics, vol. 45, no. 5, pp. 691-703.

2. **Fang Z. P., (2003),** *"Z-Source Inverter"*, IEEE Transactions on Industrial Applications, vol. 39, no. 2, pp. 504-510.

3. **Zhu Z. Q., Howe D., (2007),** *"Electrical Machines and Drives for Electric, Hybrid, and Fuel Cell Vehicles"*, Proceedings of the IEEE, vol. 95, no. 4, pp. 746-765.

4. **Shen M., Joseph A., Huang Y., Peng F. Z., Qian Z., (2006),** *"Design and Development of 50kW Z-Source Inverter for Fuel Cell Vehicles"*, IEEE Power Electronics and Motion Control Conference, vol. 2, pp.1-5.

5. **Shen M., Wang J., Joseph A., Peng F. Z., Tolbert L. M., Adams D. J., (2006),** *"Constant Boost Control of the Z-Source Inverter to Minimize Current Ripple and Voltage Stress"*, IEEE Transactions on Industrial Applications, vol. 42, No. 3, pp. 770-778.

6. **Shen M., Joseph A., Wang J., Peng F. Z., Adams D. J., (2004),** *"Comparison of Traditional Inverters and Z-Source Inverter"*, IEEE Power electronics in transportation, pp. 125-132.

7. **Farhangi B., Farhangi S., (2007),** *"Comparison of Traditional Inverters and Z-Source Inverter for Fuel Cell Vehicles"*, In IEEE Transactions on Power Electronics, vol. 22, no. 4, pp. 1453-1463.

8. **Tran Q., Chun T., Ahn J., Lee H., (2007),** *"Algorithms for Controlling Both the DC Boost and AC Output Voltage of Z-Source Inverter"*, IEEE Transactions on Industrial Electronics, vol. 54, no. 5, pp. 2745-2750.

9. **Jung J., Keyhani A., (2007),** *"Control of a Fuel Cell Based Z-Source Inverter"*, IEEE Transactions on Energy Conversion, vol. 22, no. 2, pp. 467-476.

10. **Holland K., Peng F. Z., (2005),** *"Control Strategy for Fuel Cell Vehicle Traction Drive Systems Using the Z-Source Inverter"*, IEEE Vehicle Power and Propultion, pp. 639-644.

11. **Shen M., Peng F. Z., (2006),** *"Control of the Z-Source Inverter for Fuel Cell-Battery Hybrid Vehicles to Eliminate Undesirable Operation Modes"*, IEEE Industry Applications Conference, vol. 4, pp. 1667-1673.

12. **Middlebrook R. D., Slobodan C., (1977),** *"Modeling and Analysis Methods for DC to DC Switching Converters"*, Proceedings of the International Semiconductor Power Converter Conference, pp. 90-111.

13. **Ding X., Qian Z., Xie Y., Peng F. Z., (2006),** *"A Novel Z-Source Rectifier"*, IEEE Power Electronics Specialists Conference, pp. 1-5.

14. **Sidney R. B., Yen-Shin L., (2006),** *"The Relationship Between Space Vector Modulation and Regular Sampled PWM"*, IEEE Transaction on Industrial Electronics, vol. 44, no. 5, pp.670-679.

15. **Keliang Z., Danwei W., (2007),** *"The Relationship Between Space Vector Modulation and Three Phase Carrier based on PWM:A Comprehensive Analysis"*, IEEE Transaction on Industrial Electronics, vol. 49, no. 1, pp. 186-196.

16. **Ibrahim W. I., Ismail R. M., Ghazali M. R., (2011),** *"Development of Variable Speed Drive for Single Phase Induction Motor Based on Frequency Control"*, Proceedings of Encon 4th engineering conference Kuching, Sarawak, Malaysia, vol. 19, no. 2, pp. 376-380.

17. **Lorendz R. D., (1995),** *"Tuning of Field Oriented Induction Motor Controller for High Performance Applications"*, IEEE transactions Ind. Appl., vol. 31, no. 4, pp. 812-822.

18. **Hickok H. N., (1985),** *" Adjustable Speed a Tool for Saving Energy Losses in Pumps, Fan Blower and Compressors"*, IEEE transaction industrial applications, vol. IA21, no.1, PP. 124-136.

19. **Loh P., Vilathgamuwa D. M., Gajanayake C. J., (2005),** *"Small-Signal and Signal-Flow Graph Modeling of Switched Z-Source Impedance Network"*, IEEE Power, Electronics Letters, vol. 3, no. 3, pp. 111-116.

20. **Qiu W., Kumar R., (2006),** *"Comparison of Z-Source Inverter and Boost Buck Inverter Topologies as a Single Phase Transformer-Less Photovoltaic Grid-Connected Power Conditionar"*, IEEE Power Electronics Specialist Conference, pp. 74-79.

21. **Loh P., Vilathgamuwa D. M., Gajanayake C. J., (2007),** *"Development of a Comprehensive Model and a Multiloop Controller for Z-Source Inverter DG Systems"***,** IEEE Transactions on Industrial Electronics, vol. 54, no. 4, pp. 2352-2359.

22. **Ding X., Qian Z., Yang S., Bin C., Peng F. Z., (2007),** *"A PID Control Strategy for DC link Boost Voltage in Z-Source Inverter"*, IEEE Applied Power Electronics Conference, pp. 1145-1148.

23. **Loh P., Vilathgamuwa D. M., Gajanayake C. J., (2007),** *"Transient Modeling and Analysis of Pulse-Width Modulated Z-Source Inverter"*, IEEE Transactions on Power Electronics, vol. 2, no. 22, pp. 169-177.

24. **Liu J., Hu J., Xu L., (2007),** *"Dynamic Modeling and Analysis of Z-Source Converter Derivation of AC Small Signal Model and Design-Oriented Analysis"*, IEEE Transactions on Power Electronics, vol. 22, no. 5, pp. 1786-1796.

25. **Ding X., Qian Z., Yang S., Bin C., Peng F. Z., (2007),** *"A Direct Peak DC-link Boost Control Strategy for Z-Source Inverter"*, IEEE Applied Power Electronics Conference, pp. 648-653.

26. **Zhang F., Fang X., Peng F. Z., Qian Z., (2006),** *"A New Three Phase AC-AC Z-Source Converter"*, IEEE Applied Power Electronics Conference and Exposition, pp. 123-126.

27. **Holland K., Shen M., Peng F. Z., (2005),** *"Z-source Inverter Control for Traction Drive of Fuel Cell Battery Hybrid Vehicles"*, IEEE Industrial Applications Conference, vol. 3, pp. 1651-1656.

28. **Munoz-Garcia A., Lipo T. A., Novotny D. W., (1998),** *"A New Induction Motor V/f Control Method Capable of High-Performance Regulation at Low Speeds"*, IEEE Transactions on Industry Applications, vol. 34, no. 4, pp. 813-821.

29. **Koga K., Ueda R., Sonoda T., (1992),** *"Constitution of V/f Control for Reducing the Steady-State Speed Error to Zero in Induction Motor Drive System"*, IEEE Transactions on Industry Applications, vol. 28, no. 2, pp. 463-471.

30. **Hadziselimovic M., Stumberger G., Stumberger B., Zagradisnik I., (2007),** *"Magnetically Nonlinear Dynamic Model of Synchronous Motor with Permanent Magnets"*, Journal of Magnetism and Magnetic Materials, vol. 316, pp. 257-260.

31. **Bose B. K., (2002),** *"Modern Power Electronics and AC Drives"*, Prentice Upper Saddle River, vol. 1, pp. 260-263.

APPENDICES A

CURRICULUM VITAE

PERSONAL INFORMATION
Surname, Name: SOODI, Hamed Atyia
Date and Place of Birth: 4 November 1976 , Kirkuk
Marital Status: Married
Phone: +90 538 068 51 70 / +964 770 135 88 61
Email: hamed0770@yahoo.com

EDUCATION

Degree	Institution	Year of Graduation
M.Sc.	Çankaya Univ., Electronic and Communication Engineering	2014
B.Sc.	University of Mosul, Electrical Engineering Dep., Mosul, Iraq	2002
High School	Kirkuk Preparatory School	1997

WORK EXPERIENCE

Year	Place	Enrollment
2003- 2012	Dibis Power Station, Kirkuk, Iraq	Control Engineer

FOREIGN LANGUAGES
Arabic, English, Turkish

HOBBIES

Reading, Sport, Voyage